



**A STRATEGY FOR INCLUSION OF CLOSED LOOP DYNAMICS
IN REAL TIME OPTIMIZATION**

**A STRATEGY FOR INCLUSION OF CLOSED LOOP DYNAMICS
IN REAL TIME OPTIMIZATION WITH APPLICATION
TO AN OXYGEN DELIGNIFICATION REACTOR**

by

Mohamed Soliman, B.Sc (Eng)

A Thesis
Submitted to the School of Graduate Studies
in Partial Fulfillment of the Requirements
for the Degree
Master of Applied Science

McMaster University

MASTER OF APPLIED SCIENCE (2004)
(Chemical Engineering)

McMaster University
Hamilton, Ontario, Canada

TITLE: Inclusion of Closed Loop Dynamics in Real Time Optimization
with Application to an Oxygen Delignification Reactor

AUTHOR: Mohamed Soliman, B.Sc (Eng)
(Cairo University, Egypt)

SUPERVISOR: Dr. C.L.E. Swartz

NUMBER OF PAGES: 1, 98

ABSTRACT

As driven by increasing energy costs, raw material costs and market competition, it is a necessity that modern chemical plants operate at the optimum operating point and are responsive to changes in product specification. The calculated plant optimum operating point may be at or close to constraint boundaries, which makes the process susceptible to constraint violation, off-specification products and loss of profitability in the presence of disturbances.

A new approach has been developed to track the optimum of the chemical process such that violation of constraints can be prevented by inclusion of closed loop dynamics in Real Time Optimization. Constrained model predictive control will be used as the regulatory control. This new approach introduces an additional layer in the process automation hierarchy which determines an appropriate amount of back-off from target set points based on a closed-loop dynamic model of the process. It does not require a large effort in modelling since the dynamic model is that the model used in model predictive control and the steady-state relation is the steady-state process gain of the dynamic model inside the model predictive control. It is assumed that the target set-points from the Real-Time Optimization are available to be used in our approach.

The new approach (dynamic real-time optimization) is formulated here as a multilevel program where the upper-level problem has a quadratic objective function with linear constraints and the lower-level optimization problems have quadratic objective functions that are strictly convex with linear constraints. A quadratic dynamic matrix control formulation gives rise to the lower-level optimization problems. The upper-level determines set-points that are as close as possible to set-point targets calculated at the steady-state Real-Time Optimization level, but are such that the closed loop inputs and outputs satisfy specified constraints

Oxygen bleaching in pulp mills is an example of chemical plants facing economic and environmental challenges. Improvements in the operation of oxygen delignification reactors could have a potentially significant impact on the controllability of downstream units of

the bleaching plant and the overall plant performance. Developing a dynamic model of the oxygen delignification reactor is a necessity toward meeting this objective through the development of model-based control schemes and finding the optimum set-point to the controller.

A first-principles nonlinear dynamic model of an oxygen delignification tower is developed, and used in the design and performance evaluation of a model-based control strategy. The proposed dynamic real-time optimization approach was then applied to the oxygen delignification reactor model developed to calculate the required optimum set-points by the model predictive controller in face of disturbances.

ACKNOWLEDGEMENTS

All praise are due to Allah. I thank Allah, the generous, the most compassionate and the most merciful.

I owe my deepest gratitude to my supervisor, Dr. Chris Swartz for his incessant support, patience, and understanding. His guidance and encouragement is sincerely appreciated.

Also, to the Faculty members at McMaster University, Dr. McGregor and Dr. Marlin for their assistance.

In this opportunity, I would like to acknowledge the funding from McMaster Advanced Control Consortium (MACC) throughout my studies.

I am grateful to all my friends in chemical Engineering for their support: Danielle, Honglu, Rhoda, Angela, Niki, Taufiq, Richard, Mark-John, Adam, Kevin, Jesus, Ben, Alexei, June, Koji, Pierre, Salvador, Tony, Hatopan, David, Youngsong and Manish.

Also I am grateful to my friends at Colt Engineering: Tim Giles, Tanju Cetiner and Okeef Shah for their valuable discussions and recommendations.

Finally, I am forever indebted to my wife Felicia Parker for her understanding, endless patience and love.

This thesis is dedicated to my parents, Ahmed Abd El-Rahman and Saida Gayel for their sacrifices.

Table of Contents

Table of Contents	vi
List of Figures	x
List of Tables	xiii
1 Introduction	1
1.1 Background and Motivation	1
1.2 Thesis Overview	4
2 Interaction Between RTO and MPC: Effect of Closed-Loop Dynamics	5
2.1 Introduction	5
2.2 Literature Survey	7
2.2.1 Steady-state RTO	7
2.2.2 Quadratic dynamic matrix control (QDMC)	9
2.2.3 Unconstrained model predictive control	16

2.2.4	Back-off calculations	16
2.2.5	Integration of RTO and MPC	17
2.2.6	Bilevel programming	18
2.3	Proposed Approach	21
2.3.1	Problem formulation for the constrained Case	22
2.4	Software	31
2.5	Case Studies	33
2.5.1	Isothermal CSTR	33
2.5.2	Fluid catalytic cracking unit (FCCU)	41
2.6	Future Work	49
3	Modelling of a Continuous Oxygen Delignification Unit	50
3.1	Introduction	50
3.2	Kinetic Models for Oxygen Delignification Reaction	53
3.2.1	Olm and Teder kinetic model	54
3.2.2	Hsu and Hsieh kinetic model	56
3.2.3	Myers and Edwards kinetic model	57
3.2.4	Iribarne and Schroeder model	58
3.2.5	Gendron's model	60
3.2.6	Agarwal and Genco model	61

3.2.7	Summary	62
3.3	Development of Dynamic Model for Oxygen Delignification Reactor	65
3.3.1	Assumptions and model structures	66
3.3.2	Material and energy balance	66
3.3.3	Reactor	69
3.4	Simulation Results	73
4	Model-Based Control of the Oxygen Delignification Unit	77
4.1	Introduction	77
4.2	Kushiro Mill Oxygen Bleaching Unit	77
4.2.1	Kushiro mill overview	77
4.2.2	Oxygen bleaching unit process description	78
4.3	Model-Based Control	82
4.3.1	Linear dynamic model identification	82
4.3.2	Simulation results of model-based control	83
4.3.3	Disturbance rejection	85
4.3.4	Set-point change	87
4.4	Interaction Between RTO and MPC Effect of Closed-Loop Dynamics	89
5	Conclusions and Recommendations	93
5.1	Conclusions	93

5.2 Recommendations	94
References	95

List of Figures

2.1	Optimum back-off from constraints	6
2.2	Traditional control hierarchy	8
2.3	Proposed control hierarchy	21
2.4	The multi-level optimization problem	23
2.5	Continuous stirred tank reactor(CSTR)	34
2.6	Manipulated variable is not saturated	37
2.7	Manipulated variable is touching the lower bound without saturation	38
2.8	Manipulated variable is partially saturated	39
2.9	Manipulated variable is completely saturated	40
2.10	Fluid catalytic cracking unit (FCCU)	41
2.11	Schematic of model predictive control problem for the catalytic cracking reactor-regenerator system	42
2.12	Effect of small disturbances on the manipulated and controlled variables	46
2.13	Both of the manipulated variables are partially saturated	47

2.14 Both of the manipulated variables are saturated	48
3.1 Comparison of the different models operating ranges	63
3.2 Modeling oxygen delignification reactor as a series of n CSTRs	65
3.3 Feed Mixer	67
3.4 Step response of the outlet kappa number and outlet viscosity to step disturbance in the delignification reactor top temperature ($\Delta T = -5K$)	74
3.5 Step responses of the outlet kappa number and outlet viscosity to step disturbance in the delignification reactor inlet kappa number ($\Delta kappa = +5$)	75
3.6 Step response of the outlet kappa number and outlet viscosity to +4 kg/ton change in the delignification reactor inlet caustic flow rate	76
4.1 Jujo Mill oxygen bleaching line	79
4.2 Model Predictive control simulation using a nonlinear plant	83
4.3 Closed-loop responses of the outlet kappa number and outlet viscosity, for step disturbances in the delignification reactor inlet kappa number (+3)	85
4.4 Closed-loop responses of the outlet kappa number and outlet viscosity, for step disturbances in the delignification reactor inlet kappa number (-3)	86
4.5 Closed-loop responses of the outlet kappa number and outlet viscosity, for set-point change of +1 in the outlet kappa number	87
4.6 Closed-loop responses of the outlet kappa number and outlet viscosity, for set-point change of +0.5 in the outlet kappa number and -0.5 cP in the outlet viscosity	88

4.7	Non of the manipulated variables are saturated	91
4.8	Output response to a step change in inlet kappa number of 2.82.	92

List of Tables

2.1	MPC tuning parameters	35
2.2	Comparison of the different solvers	36
2.3	MPC tuning parameters	45
3.1	Summary of global kinetic models	64
4.1	Jujo Mill oxygen bleaching line operating conditions	80
4.2	MPC tuning parameters	84
4.3	MPC tuning parameters	89

Chapter 1

Introduction

1.1 Background and Motivation

As driven by increasing energy costs, restrictive environmental regulations, changing raw material prices, quality specifications, market demands, changes in equipment and so forth, the operating point of a plant will not remain constant. It is then a necessity for modern chemical plants to operate at the optimum operating point and be responsive to product specification.

For maximizing the profit of any chemical process, it has to have excellent dynamic performance and it should be maintained at or near a steady-state. Model predictive control is used to obtain an excellent dynamic performance and maintain the process operating close to the set-points. This is achieved by calculating the predicted manipulated variable moves and the predicted output variables over a time interval. Real-Time Optimizers (RTO) are often used with explicit economics for the calculation of the set-points. The calculated plant optimum may be at or close to constraint boundaries, which makes the process susceptible to constraint violation in the presence of disturbances.

Traditionally, research has focused on using back-off methods. However, if the back-off is larger than necessary, the constraints will not be violated but the loss of profits increases. On

the other hand, if the back-off is less than necessary, infeasible operation will result. Some other work has been done to integrate real-time optimization into linear model predictive controllers in order to rapidly accommodate measured disturbances while avoiding offsets. However, extending model predictive control to include a nonlinear steady-state to predict the optimal operational point will lead to a complex optimization problem and the plant can become unstable if the numerical algorithm used to solve the controller optimization problem fails to converge.

The goal of this work is to develop a method to track the optimum of the chemical process such that violation of constraints can be prevented (dynamic real-time optimization) by inclusion of closed loop dynamics in Real Time Optimization. Constrained model predictive control will be used as the regulatory control.

In the new approach, the MPC and steady-state RTO layers are kept separate, but a new layer introduced between them to estimate the necessary back-off on the basis of the predicted closed loop response to expected disturbances. This new approach simplifies the previously proposed automation structures by removing the dynamics from RTO and economics from MPC. No Real Time Optimization calculations will be done. It is assumed that the target set-points from the RTO are available to be used in our approach.

The Dynamic Real-Time Optimization (DRTO) problem is formulated here as a multilevel program where the upper and lower-level problems have a quadratic objective function with linear constraints. A QDMC controller formulation is used as the lower-level optimization problems. The DRTO level determines set-points that are as close as possible to set-point targets calculated at the steady-state RTO level, but are such that the closed loop inputs and outputs satisfy specified constraints.

Oxygen bleaching in pulp mills is an example of chemical plants facing economic and environmental challenges. Improvements in the operation of oxygen delignification reactors could have a potentially significant impact on the controllability of downstream units of the bleaching plant and the overall plant performance. A problem that needs to be taken into account in the operation of oxygen delignification units is the natural tendency of oxygen

to form reactive free radicals that can attack cellulose and other carbohydrates in addition to the lignin that is required to be broken down. This adversely affects pulp strength, and consequently poses a constraint on operation of the process.

A fundamental, nonlinear dynamic model that predicts cellulose degradation and lignin removal over a wide range of operating conditions should permit oxygen delignification units to be run such that lignin is removed to the farthest extent while maintaining an acceptable level of pulp strength. Developing a dynamic model of the oxygen delignification reactor is a necessity toward meeting this objective through the use of model-based control schemes, and finding the optimum set-point to the controller using the Dynamic Real Time Optimization approach(DRTO).

A first-principles nonlinear dynamic model of an oxygen delignification tower is developed incorporating literature-based kinetic models for prediction of the kappa number and pulp viscosity. Through the literature review, models proposed by Iribarne and Schroeder [1997] and Myers and Edwards [1989] were found to be the most suitable for many processes because they cover a wide range of operating conditions. The Myers and Edwards [1989] model was used to describe lignin removal and the Iribarne and Schroeder [1997] model to describe the cellulose degradation, and used in the design and performance evaluation of a model-based control strategy. The effect of process disturbances on the optimum operating point of the plant has also been explored.

Model predictive control studies were conducted using the Matlab MPC Toolbox for the nonlinear oxygen delignification plant model developed in Simulink as S-functions. The control objective was to maintain the outlet kappa number and viscosity at their set points by manipulating the reactor temperature set point and inlet caustic rate. The reactor temperature is being controlled using a local PID controller by manipulating the steam flow rate. Disturbances considered were changes in the inlet kappa number of the pulp feed. Step tests were performed on the model, and linear dynamic relationships between the inputs and outputs were identified. The Dynamic Real Time Optimization approach was then used to calculate the set-points to the MPC.

1.2 Thesis Overview

Chapter 2 – Interaction Between RTO and MPC. Effect of Closed-Loop Dynamics

In Chapter 2, a method to track the optimum of the chemical process such that violation of constraints can be prevented (Dynamic Real-Time Optimization) is developed. A literature survey is first presented followed by a Mixed Integer Quadratic Programming (MIQP) optimization formulation of the DRTO problem. A fluid catalytic cracking unit is then presented as a case study to illustrate the proposed DRTO approach.

Chapter 3 – Modelling of a Continuous Oxygen Delignification Unit

This chapter describes the development of a dynamic model of an oxygen delignification unit. The model is based on fundamental mass and energy balances, and incorporates literature-based kinetic models for prediction of the kappa number and pulp viscosity. The development of the model is described. It is then used to generate open-loop responses which are briefly explained.

Chapter 4 – Model-Based Control Of the Oxygen Delignification Unit

Chapter 4 describes the model-based control strategies for oxygen delignification unit. The dynamic model developed in chapter 3 is used to generate an approximate linear dynamic model for use in a model-based control strategy. This involves QDMC with DRTO used to determine the set-points

Chapter 5 – Conclusions and recommendations

Chapter 5 will conclude with a summary of the presented methods and investigation results of both case-studies in the preceding chapters. Based on these conclusions, some recommendations for future work will also be discussed.

Chapter 2

Interaction Between RTO and MPC: Effect of Closed-Loop Dynamics

2.1 Introduction

Processes are always subject to disturbances. These disturbances can lead to off-specification products, loss of profitability and constraint violations that result in unsafe plant conditions. For maximizing the profit of any chemical process, it has to have excellent dynamic performance and it should be maintained at or near a steady-state. Model predictive control is often used to obtain an excellent dynamic performance and maintain the process operating close to the set-points. This is achieved by calculating the predicted manipulated variable moves and the predicted output variables over a time interval. Real-Time Optimizers (RTO) are often used with explicit economics for the calculation of the set-points.

Motivation and goals

RTO based on a steady-state nonlinear model is typically used to calculate the optimum process operating point. However, steady state RTO has some deficiencies. First, it can

handle only low frequency disturbances. Second, for low frequency disturbances, the calculated plant optimum may be at or close to constraint boundaries, which makes the process susceptible to constraint violation in the presence of disturbances.

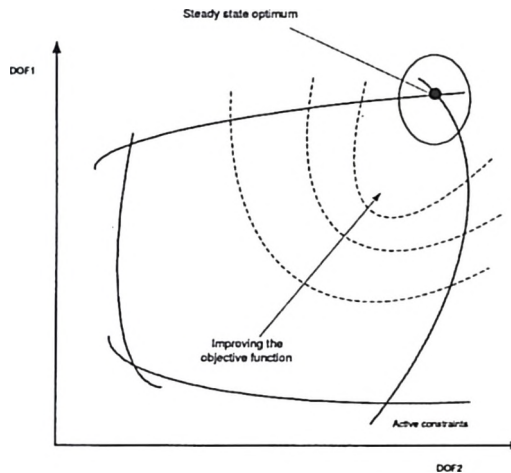


Figure 2.1: Optimum back-off from constraints

Traditionally, research has focused on using back-off methods. However, if the back-off is larger than necessary, the constraints will not be violated but the loss of profits increases. On the other hand, if the back-off is less than necessary, infeasible operation will result.

The goal of this work is to develop a method to track the optimum of the chemical process such that violation of constraints can be prevented (dynamic real-time optimization). Constrained model predictive control will be used as the regulatory control.

Main contribution

In our approach, we will keep both RTO and MPC layers separate to take full advantage of their characteristics. A linear dynamic model, the same linear model inside the MPC, will be used to calculate the optimal amount of back-off. The resulting optimization problem is challenging because it is a multi-level optimization problem which is not trivial to solve. However, the solution approach followed will guarantee global optimality .

2.2 Literature Survey

2.2.1 Steady-state RTO

Due to the increasing energy cost, restrictive environmental regulations, changing raw material prices, quality specifications, market demands, changes in equipment and so forth, the operating point of a plant will not remain constant. Due to the fact that improving the plant operation is much cheaper than building new plants, optimization is used to achieve these improvements in the process. This involves the manipulation of the degrees of freedom of the process to satisfy the plant economic objectives.

Chemical processes are always subject to high frequency disturbances which will be rejected by regulatory control, while the low frequency disturbances shift the optimal operating point ; thus new optimal operating conditions must be established. RTO is then used to calculate this new optimum.

Steady-state optimization (RTO) is used when the frequency of non-stationary disturbances is smaller than the frequency of the optimization runs and the time between the optimization runs is sufficient for the plant to reach the new steady-state [Kassidas, 1993]. Real-time optimization is the level in the control hierarchy at which business decisions are integrated into the process operation. This linking of economic and process effects provides a powerful tool for maximizing the operating profitability.

Traditional control hierarchy

The traditional control hierarchy consists of four levels as follows:

1. Plant scheduling
2. Steady-state optimizer (RTO): Calculates the optimal operating conditions and sends the set-points either to the advanced controller in the level below or directly to the regulatory PID control layer. Nath and Alzein [2000] presented a typical RTO execution cycle illustrated in the Figure 2.2 as the following:

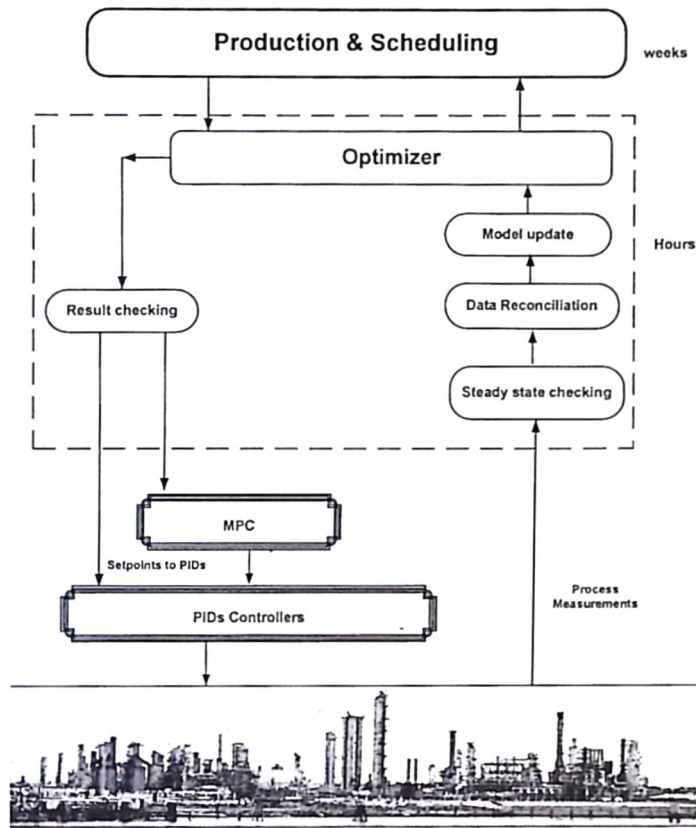


Figure 2.2: Traditional control hierarchy

- (a) Steady-state detection of the process: This is to ensure that the process is close to or at steady-state; furthermore, the current process data can be used to establish the initial state of the process.
- (b) Data reconciliation and parameter estimation: The purpose of this step is to reconcile the process data and to determine the model parameters that best fit the process state established in the previous step.
- (c) Optimization of the updated model.
- (d) Consistency check before downloading the data to the underlying control layer. This step is used to evaluate the change in the profit from the current to the

new conditions. If the increase is not significant, the new conditions will not be implemented in the plant.

3. Advanced controller (Model predictive controller): Acting as a constrained controller, it receives the set-point from the RTO layer to calculate the set-point for the regulatory PID control layer below.
4. Regulatory control layer (PID): Receives its set-points from the RTO layer or the MPC layer and directly manipulates the process valves.

Deficiencies of traditional control hierarchy

The traditional control hierarchy suffers from two major deficiencies:

1. The steady-state detection step of RTO may take a very long time, depending on the process, which means holding the set-points constant for a long time which will result in loss in profit. This deficiency is handled in literature as a **profit controller**, optimizer controller or integration of real-time optimization (RTO) into MPC [Zanin *et al.*, 2002] and [Becerra *et al.*, 1998].
2. The calculated optimal set-points sent to the controller may lie at or close to the process constraints; consequently constraint violation will occur in the presence of disturbances.

2.2.2 Quadratic dynamic matrix control (QDMC)

Model Predictive Control (MPC) has within the past two decades become the advanced control strategy of choice within the chemical process industry. Key features are that it accommodates process interactions and dead time directly, and that constraints on manipulated inputs and process outputs are handled explicitly. The latter feature is particularly important in real-time optimization, since the steady-state economic optimum generally lies at the intersection of one or more process constraints. The MPC algorithm uses a dynamic model to predict future outputs based on future input changes over a specified time horizon.

Model Predictive Control (MPC) refers to a class of computer control algorithms that utilize an explicit process model to predict the future response of a plant to changes in the manipulated variables u over prediction horizon P at the present time k . At each control interval an MPC algorithm attempts to optimize future plant behavior by computing a sequence of a future manipulated variable adjustments. Only the first computed change in the manipulated variable Δu is implemented. At time $k + 1$ the computation is repeated with the horizon moved by one time interval. The discrepancy between the predicted and measured outputs is used to adjust the model predictions. Comprehensive descriptions of MPC are given in Qin and Badgwell [2003] and Bequette [2000].

From among the various MPC algorithms which include Model Algorithmic Control (MAC), Dynamic matrix control(DMC), Generalized Predictive Control (GPC),etc, QDMC based on a step response model will be used. Constraints on manipulated inputs will be considered.

The QDMC algorithm as presented by Bequette [2000] and Garcia and Morshedi [1986] will be used in this study. QDMC (Quadratic Dynamic Matrix Control) consists of the on-line solution of a quadratic program which minimizes the sum of squared deviations of controlled variables from their set-points subject to the controlled variables being within their bounds. QDMC for single-input single-output systems can be written in matrix-vector form at step k as follows:

$$\min_{\Delta u_{k+i|k}} \frac{1}{2} \begin{bmatrix} y_{sp} - \hat{y}_{k+1|k} \\ y_{sp} - \hat{y}_{k+2|k} \\ \vdots \\ y_{sp} - \hat{y}_{k+P|k} \end{bmatrix}^T \Gamma^T \Gamma \begin{bmatrix} y_{sp} - \hat{y}_{k+1|k} \\ y_{sp} - \hat{y}_{k+2|k} \\ \vdots \\ y_{sp} - \hat{y}_{k+P|k} \end{bmatrix} - \begin{bmatrix} \Delta u_{k|k} \\ \Delta u_{k+1|k} \\ \vdots \\ \Delta u_{k+M-1|k} \end{bmatrix}^T \Lambda^T \Lambda \begin{bmatrix} \Delta u_{k|k} \\ \Delta u_{k+1|k} \\ \vdots \\ \Delta u_{k+M-1|k} \end{bmatrix} \quad (2.1)$$

Subject to

$$\begin{bmatrix} 1 & 0 & \cdots & 0 \\ 1 & 1 & \cdots & 0 \\ \vdots & \vdots & & \\ 1 & 1 & \cdots & 1 \end{bmatrix} \begin{bmatrix} \Delta u_{k|k} \\ \Delta u_{k+1|k} \\ \vdots \\ \Delta u_{k+M-1|k} \end{bmatrix} \geq \begin{bmatrix} u_{min} - u_{k-1} \\ u_{min} - u_{k-1} \\ \vdots \\ u_{min} - u_{k-1} \end{bmatrix} \quad (2.2)$$

$$- \begin{bmatrix} 1 & 0 & \cdots & 0 \\ 1 & 1 & \cdots & 0 \\ \vdots & \vdots & & \\ 1 & 1 & \cdots & 1 \end{bmatrix} \begin{bmatrix} \Delta u_{k|k} \\ \Delta u_{k+1|k} \\ \vdots \\ \Delta u_{k+M-1|k} \end{bmatrix} \geq \begin{bmatrix} u_{k-1} - u_{max} \\ u_{k-1} - u_{max} \\ \vdots \\ u_{k-1} - u_{max} \end{bmatrix} \quad (2.3)$$

$$\begin{bmatrix} \Delta u_{min} \\ \Delta u_{min} \\ \vdots \\ \Delta u_{min} \end{bmatrix} \leq \begin{bmatrix} \Delta u_{k|k} \\ \Delta u_{k+1|k} \\ \vdots \\ \Delta u_{k+M-1|k} \end{bmatrix} \leq \begin{bmatrix} \Delta u_{max} \\ \Delta u_{max} \\ \vdots \\ \Delta u_{max} \end{bmatrix} \quad (2.4)$$

$$\begin{bmatrix} y_{min} \\ y_{min} \\ \vdots \\ y_{min} \end{bmatrix} \leq \begin{bmatrix} \hat{y}_{k+1|k} \\ \hat{y}_{k+2|k} \\ \vdots \\ \hat{y}_{k+P|k} \end{bmatrix} \leq \begin{bmatrix} y_{max} \\ y_{max} \\ \vdots \\ y_{max} \end{bmatrix} \quad (2.5)$$

It is clear that the above problem (2.1 to 2.5) can not be solved without prediction of the future output $\hat{y}_{k+\ell|k}$. This, in turn, necessitates the availability of a process model which is considered to be the heart of MPC controllers. The step response model for a single-input single-output system is considered.

$$y_k = S_1\Delta u_{k-1} + S_2\Delta u_{k-2} + \cdots + S_{N-1}\Delta u_{k-N+1} + S_N u_{k-N} + d_k \quad (2.6)$$

which can be written in the form

$$y_k = \sum_{i=1}^{N-1} S_i \Delta u_{k-i} + S_N u_{k-N} + d_k \quad (2.7)$$

where S_i are the step response coefficients, y_k is the model prediction at time step k , N is the number of steps to steady-state, and u_{k-N} is the manipulated input N steps in the past. The model predicted output y_k is unlikely to be equal to the actual measured output y_k^m at the time step k . The difference between the measured output and the model prediction is called the additive disturbance d_k . Using the step response model to predict the outputs over the prediction horizon P gives:

$$\begin{aligned}
 \begin{bmatrix} \hat{y}_{k+1|k} \\ \hat{y}_{k+2|k} \\ \hat{y}_{k+3|k} \\ \vdots \\ \hat{y}_{k+P|k} \end{bmatrix} &= \underbrace{\begin{bmatrix} S_1 & 0 & \cdots & 0 & 0 \\ S_2 & S_1 & \cdots & 0 & 0 \\ S_3 & S_2 & \cdots & 0 & 0 \\ \vdots & \vdots & & & \\ S_P & S_{P-1} & \cdots & S_{P-M+2} & S_{P-M+1} \end{bmatrix}}_{y^P : \text{Effect of current and future control moves}} \begin{bmatrix} \Delta u_{k|k} \\ \Delta u_{k+1|k} \\ \Delta u_{k+2|k} \\ \vdots \\ \Delta u_{k+M-1|k} \end{bmatrix} \\
 &+ \underbrace{\begin{bmatrix} S_2 & S_3 & \cdots & S_{N-2} & S_{N-1} \\ S_3 & S_4 & \cdots & S_{N-1} & 0 \\ S_4 & S_5 & \cdots & 0 & 0 \\ \vdots & \vdots & & & \\ S_{P+1} & S_{P+2} & \cdots & 0 & 0 \end{bmatrix}}_{y^* : \text{Effect of past control moves}} \begin{bmatrix} \Delta u_{k-1|k} \\ \Delta u_{k-2|k} \\ \Delta u_{k-3|k} \\ \vdots \\ \Delta u_{k-N+2|k} \end{bmatrix} + \underbrace{S_N}_{S_N} \begin{bmatrix} u_{k-N+1|k} \\ u_{k-N+2|k} \\ u_{k-N+3|k} \\ \vdots \\ u_{k-N+P|k} \end{bmatrix} \quad (2.8) \\
 &+ \underbrace{\begin{bmatrix} \hat{d}_{k+1|k} \\ \hat{d}_{k+2|k} \\ \hat{d}_{k+3|k} \\ \vdots \\ \hat{d}_{k+P|k} \end{bmatrix}}_{\text{Predicted disturbance}}
 \end{aligned}$$

or it can be simplified as follows:

$$\hat{y}_k = A\Delta u_k + y_k^* + \hat{d}_k \quad (2.9)$$

The prediction of the output in Equation 2.9 and 2.8 involves three terms on the right-hand side. The first term ($A\Delta u_k$) includes the present and all future moves of the manipulated variables which are to be determined so as to minimize the objective function (2.1). The second term y_k^* includes only past values of the manipulated variables and is completely known at time k . The third term \hat{d}_k is the predicted disturbance which is commonly assumed constant for all future times $\ell \geq 0$.

$$\hat{d}_{k|k} = \hat{d}_{k+1|k} = \cdots = \hat{d}_{k+\ell|k} \quad (2.10)$$

At time k , the disturbance is estimated as the difference between the measured output y_k^m and the output predicted from the model.

$$\hat{d}_{k|k} = y_k^m - \hat{y}_{k|k} \quad (2.11)$$

Also beyond the the control horizon M , there are no control moves

$$\Delta u_{k+M|k} = \Delta u_{k+M+1|k} = \Delta u_{k+M+2|k} = \dots = \Delta u_{k+P-1|k} = 0 \quad (2.12)$$

By substituting Equation 2.9 into Equation 2.1, the following quadratic program (QP) results:

$$\begin{aligned} \min_{\Delta \mathbf{u}_k} & \frac{1}{2} \Delta \mathbf{u}_k^T H \Delta \mathbf{u}_k + \mathbf{g}_k^T \Delta \mathbf{u}_k \\ \text{s.t.} & \quad I_L \Delta \mathbf{u}_k \leq \mathbf{u}_{max} - u_{k-1} \mathbf{e} \\ & \quad -I_L \Delta \mathbf{u}_k \leq -\mathbf{u}_{min} + u_{k-1} \mathbf{e} \\ & \quad \Delta \mathbf{u}_{min} \leq \Delta \mathbf{u}_k \leq \Delta \mathbf{u}_{max} \\ & \quad \mathbf{g}_k = A^T \Gamma^T \Gamma (\mathbf{y}_k^* + \hat{\mathbf{d}}_k - \mathbf{y}_{sp}) \\ & \quad \hat{\mathbf{y}}_k = \mathbf{y}_k^* + \hat{\mathbf{d}}_k + A \Delta \mathbf{u}_k \\ & \quad \mathbf{y}_{min} \leq \hat{\mathbf{y}}_k \leq \mathbf{y}_{max} \end{aligned} \quad (2.13)$$

where:

$$I_L = \begin{bmatrix} 1 & 0 & 0 & 0 & \dots & 0 & 0 \\ 1 & 1 & 0 & 0 & \dots & 0 & 0 \\ \vdots & \vdots & \vdots & \vdots & & \vdots & \vdots \\ 1 & 1 & 1 & 1 & \dots & 1 & 1 \end{bmatrix}_{(M \times M)} \quad (2.14)$$

and

$$\mathbf{e} = \begin{bmatrix} 1 & 1 & 1 & 1 & \dots & 1 & 1 \end{bmatrix}_{(1 \times M)}^T \quad (2.15)$$

$\hat{y}_k =$ A vector that represents the predicted value of y at time $k + \ell$ based on information available at time k taking into account the effect of the future and past control moves.

$u_k =$ A vector of future control values with respect to which the optimization will be performed

$$\Delta u_{k+i|k} = u_{k+i|k} - u_{k+i-1|k}$$

$y_{sp} =$ The set-point vector

$\Gamma =$ The matrix that contains the weights on the controlled variables

$\Lambda =$ Manipulated variables weighting matrix

$P =$ The prediction horizon

$M =$ The control horizon

H is the Hessian matrix and it is constant,

$$H = A^T \Gamma^T \Gamma A + \Lambda^T \Lambda \quad (2.16)$$

and A is called the dynamic matrix of the system, defined as

$$A = \begin{bmatrix} S_1 & 0 & \cdots & 0 & 0 \\ S_2 & S_1 & \cdots & 0 & 0 \\ S_3 & S_2 & \cdots & 0 & 0 \\ \vdots & \vdots & & & \\ S_{P-1} & S_{P-2} & \cdots & S_{P-M+1} & S_{P-M} \\ S_P & S_{P-1} & \cdots & S_{P-M+2} & S_{P-M+1} \end{bmatrix} \quad (2.17)$$

while g_k is the gradient vector and it needs to be updated every time step.

$$\begin{bmatrix} g_{k+1|k} \\ g_{k+2|k} \\ \vdots \\ g_{k+P|k} \end{bmatrix} = A^T \Gamma^T \Gamma \left(\begin{bmatrix} y_{k+1|k}^* \\ y_{k+2|k}^* \\ \vdots \\ y_{k+P|k}^* \end{bmatrix} + \begin{bmatrix} d_{k|k} \\ d_{k|k} \\ \vdots \\ d_{k|k} \end{bmatrix} - \begin{bmatrix} y_{sp} \\ y_{sp} \\ \vdots \\ y_{sp} \end{bmatrix} \right) \quad (2.18)$$

where \mathbf{y}_k^* is a vector of the model predicted output provided no moves are made at time $k, k+1, k+2, \dots$; which means that u_{k-1} is kept constant over a prediction horizon P .

$$\begin{bmatrix} y_{k+1|k}^* \\ y_{k+2|k}^* \\ y_{k+3|k}^* \\ \vdots \\ y_{k+p|k}^* \end{bmatrix} = \begin{bmatrix} S_2 & S_3 & \cdots & S_{N-2} & S_{N-1} \\ S_3 & S_4 & \cdots & S_{N-1} & 0 \\ S_4 & S_5 & \cdots & 0 & 0 \\ \vdots & \vdots & & & \\ S_{P+1} & S_{P+2} & \cdots & 0 & 0 \end{bmatrix} \begin{bmatrix} \Delta u_{k-1|k} \\ \Delta u_{k-2|k} \\ \Delta u_{k-3|k} \\ \vdots \\ \Delta u_{k-N+2|k} \end{bmatrix} + S_N \begin{bmatrix} u_{k-N+1|k} \\ u_{k-N+2|k} \\ u_{k-N+3|k} \\ \vdots \\ u_{k-N+P|k} \end{bmatrix} \quad (2.19)$$

In a typical MPC fashion [Garcia *et al.*, 1989], the above optimization problem is solved at time k . At the present time k , the behavior of the process over a horizon P is considered. Using a model, the process response to changes in the manipulated variables is predicted. The moves of the manipulated variables are selected such that the predicted response has desirable characteristics. Only the first computed change in the manipulated variables is implemented. At time $k+1$, the computation is repeated with horizon moved by one time interval. The procedure is repeated at times $k+2, k+3, \dots$.

2.2.3 Unconstrained model predictive control

When there are no inequality constraints for the manipulated variables and the controlled variables in Equation 2.13, it will reduce to unconstrained optimization problem, which has the following analytical solution:

$$\Delta \mathbf{u}_k = (A^T \Gamma^T \Gamma A + \Lambda^T \Lambda)^{-1} A^T \Gamma^T \Gamma (\mathbf{y}_{sp} - \mathbf{y}_k^* - \hat{\mathbf{d}}_k) \quad (2.20)$$

2.2.4 Back-off calculations

Chemical plants are always subject to disturbances which shift the plants from operating at the optimal point, leading to potential constraint violations. Some work has been done

previously on handling these constraint violations. Bandoni *et al.* [1994] presented an algorithmic approach for determining the necessary back-off from the steady-state optimum. This work focused on moving the steady-state operating point sufficiently far from active constraints into the feasible region to ensure there are no constraint violations during the plant operation.

Average deviation from the true optimum is another way of backing the calculated set-point away from the active constraints. The calculated optimum back-off will depend on the parametric uncertainty, measurement error and model mismatch. It is based on a first and second order Taylor series expansion of a rigorous and approximate optimization model [Loeblein and Perkins, 1996].

2.2.5 Integration of RTO and MPC

Including RTO within MPC (Optimizing Controller)

Based on the fact that there are some plants that are continuously perturbed and take a long time to reach steady-state, several researchers have attempted to integrate an economic objective into MPC formulations to avoid long waits to reach steady-state. Zanin *et al.* [2002] integrated real-time optimization into linear model predictive controllers in order to rapidly accommodate measured disturbances while avoiding offsets for a fluid catalytic cracking (FCC) unit. They pointed out that the traditional control hierarchy has a major deficiency; both the controller and the optimizer are not dealing with the same pieces of information which may result in the predicted optimal operational point being suboptimal. However, extending model predictive control to include a nonlinear steady-state to predict the optimal operational point will lead to a complex optimization problem and the plant can become unstable if the numerical algorithm used to solve the controller optimization problem fails to converge. Furthermore, it is difficult to update the steady-state model to reflect the real process.

Including MPC dynamics within the RTO level

Loeblein and Perkins [1999] calculated the effect of disturbances on the outputs through the closed loop system using the unconstrained model predictive control law, so the amount of back-off from the constraints that guarantees the feasible operation of the process can be determined.

On the other hand, Brengel and Seider [1992] did some similar work applying it to the integration of process design and process control. They integrated the plant design and control problem and solved the problem simultaneously to come up with an operationally optimal plant design. They used the nonlinear model predictive controller to reject the disturbances. Their algorithm does not guarantee global optimality.

2.2.6 Bilevel programming

A bilevel programming problem results when only two levels of interactions are considered. Mathematically, it can be formulated as follows using the same notation of Clark and Westerberg [1990]. Uppercase letters refer to the first level (outer problem) and lowercase letters refer to 2nd level (inner problem).

$$\begin{aligned}
 & \min_x F(x, y) \\
 & \text{subject to } H(x, y) = 0 \\
 & \quad G(x, y) \leq 0 \\
 & \quad \min_y f(x, y) \\
 & \quad \text{subject to } h(x, y) = 0 \\
 & \quad \quad g(x, y) \leq 0
 \end{aligned} \tag{2.21}$$

In equations 2.21, the outer optimizer selects values for the variables x , and given these values, the inner optimizer selects the values of the variables y that minimize the inner

problem objective f but the y variables affect the outer problem as well.

Difficult characteristic of the bilevel program Bilevel programs are considerably more difficult than single-level optimizations because of interactions between the inner and outer optimizers. The outer problem sets parameters influencing the inner optimization, but the outer optimization, in turn, is affected by the outcome of the inner problem. These interactions lead to serious problems, such as multiple inner problem optima, loss of convexity and differentiability. These difficulties are illustrated below.

1. **Multiple inner problem minima:** If the inner problem has multiple minima for certain values of the outer problem variables x , there is no specific requirement in the statement of the bilevel program that any particular solution can be chosen. However, the outer objective F will, in general, be a function of the inner variables as well and will not have the same values for all inner minima. The outer optimizer will choose any point of the inner optimizer's feasible solutions sets that satisfy the outer constraints (global solution).
2. **Non-convexity:** Even if each level of the bilevel problem is convex (global optimum can be found), the resulting bilevel problem combining the two is generally a nonconvex program.
3. **Non-differentiability:** The best algorithm for single-level nonlinear programs uses gradient information to build local approximations and iterate to improve the estimate of the solution [Kassidas, 1993]. As the outer variables are adjusted, there may be changes in the set of active inequalities of the inner problem optimum. At the boundary points where these changes occur, the equality constraints that are introduced by the inner problem's requirement for optimality, have no derivatives. Algorithms that use gradient information will fail at these points; therefore, an explicit enumeration technique is required to consider all the possible directions and choose a descent direction for the outer problem, while maintaining the inner problem optimality [Clark and Westerberg, 1990]. This non-differentiability arises from the interaction of the On/Off nature of the complimentary constraints with the stationary relationships.

4. Degeneracy: - Redundant inner program constraints

In algorithms for single-level mathematical programs, redundant constraints are located during the solution process and discarded. In a bilevel program, however the parametric nature of the inner optimization poses the problem of degeneracy. For some values of the of the outer variables, some inner constraints may be redundant at the inner problem optimum, therefore they could be deactivated and allow the outer objective F to improve.

Solution algorithms for the bilevel programming problem

Many different algorithms have been developed to compute the global optimum of this problem. There are two main algorithms for solving a general bilevel program. The first approach comprises penalty methods that have played a key role beginning in the early 1980s. It approximates the original two-level problem as series of a single-level nonlinear programs [Bard, 1998].

The second approach is based on solving the nonlinear program obtained by replacing the lower-level problems by its Karush–Kuhn–Tucker conditions. Bard [1998] applied an active constraint strategy and replaced the lower-level problem with its stationary conditions. Fortuny-Amat and McCarl [1981] developed a computational method by transforming the original problem into a mixed-integer program. Bard and Moore [1990] developed a branch and bound algorithm for linear/quadratic problems by exploiting Karush–Kuhn–Tucker conditions associated with the inner problem.

2.3 Proposed Approach

RTO is usually executed every few hours. It is used to handle the non-stationary disturbances with frequencies lower than the execution frequency of the RTO and the critical frequency of slowest control loops.

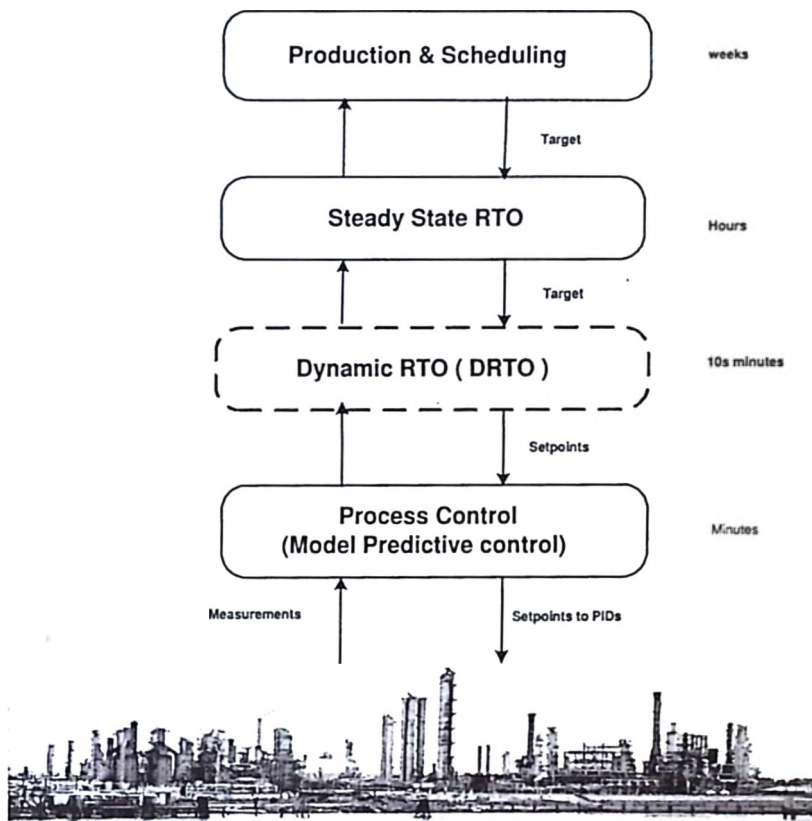


Figure 2.3: Proposed control hierarchy

RTO usually assumes perfect control in the controller layer so the disturbance is perfectly rejected which is not the case in reality. RTO predicts the steady-state optimum which is generally at or close to constraints. In the presence of the disturbances, the constraints will be violated. Consequently, some work has been done to incorporate the control into

RTO layer to take into account the dynamics. Involving the dynamics into the RTO layer makes it a more complex problem that takes a longer time to solve with no guarantee for a global optimum or even finding a solution. Another approach followed is to incorporate the economics into the controller level, but this makes the problem more complex, causing it to take long time to be solved and still with no guarantee for global optimum or even a solution Zanin *et al.* [2002].

In this work a new approach is proposed to handle these problems. The MPC and steady-state RTO layers are kept distinct, but a new layer inserted between them to determine the necessary back-off on the basis of the predicted closed loop response to expected disturbances. This new approach simplifies the previously proposed automation structures by removing the dynamics from RTO and economics from MPC. This new layer will not require a large effort in modelling. The dynamic model will be the model used in MPC and the steady-state relation will be the steady-state process gain of the dynamic model inside the MPC controller.

2.3.1 Problem formulation for the constrained Case

Multilevel optimization problem

In this section, the problem formulation for single-input single-output systems is presented. This formulation can be easily extended to the multiple-input multiple-output case.

The dynamic real-time optimization (DRTO) problem is formulated here as a multilevel program where the upper and lower-level problems have a quadratic objective function with linear constraints and the lower-level optimization problems (controller 1 to controller N_s) have quadratic objective functions that are strictly convex with linear constraints. A QDMC controller formulation is used as the lower-level optimization problems. Constraints on the magnitude of the control changes and hard output constraints will not be considered within the MPC controller. Constraints on the outputs are accommodated at the outer optimization level through adjustments of the set-point. The formulation is illustrated

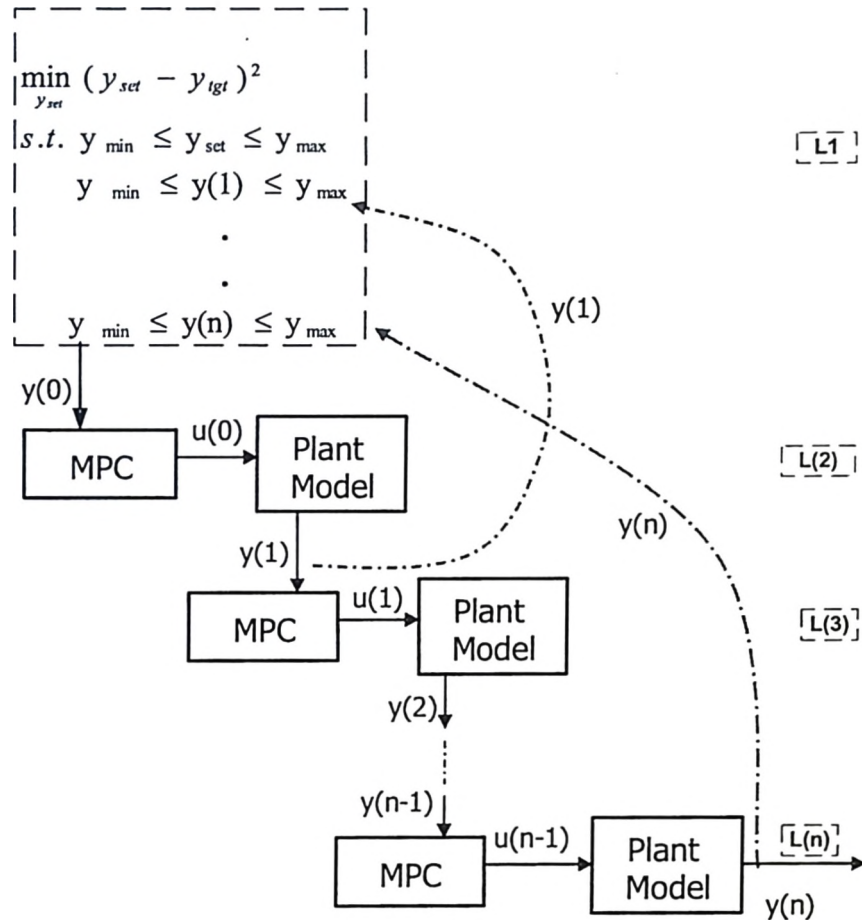


Figure 2.4: The multi-level optimization problem

schematically in Figure 2.4. The DRTO level determines set-points that are as close as possible to set-point targets calculated at the steady-state RTO level, but are such that the closed loop inputs and outputs satisfy specified constraints. The QDMC problem at time step k will be as follows:

$$\begin{aligned}
 & \min_{\Delta \mathbf{u}_k} \frac{1}{2} \Delta \mathbf{u}_k^T H \Delta \mathbf{u}_k + \mathbf{g}_k^T \Delta \mathbf{u}_k \\
 & \text{s.t.} \quad I_L \Delta \mathbf{u}_k \leq \mathbf{u}_{max} - u_{k-1} \mathbf{e} \\
 & \quad \quad -I_L \Delta \mathbf{u}_k \leq -\mathbf{u}_{min} + u_{k-1} \mathbf{e} \\
 & \quad \quad \mathbf{g}_k = A^T \Gamma^T \Gamma (\mathbf{y}_k^* + \hat{\mathbf{d}}_k - \mathbf{y}_{sp})
 \end{aligned} \tag{2.22}$$

$$\hat{\mathbf{y}}_k = \mathbf{y}_k^* + \hat{\mathbf{d}}_k + A \Delta \mathbf{u}_k \tag{2.23}$$

The resulting multi-level optimization problem for SISO systems is:

$$\min_{y_{sp}} (y_{sp} - y_{tgt})^2 \tag{2.24}$$

Subject to

$$u_{ss} = a y_{sp} + b \tag{2.25}$$

$$y_{min} \leq y_{sp} \leq y_{max} \tag{2.26}$$

$$\text{Controller 1} \tag{2.27}$$

$$\text{Model output 1} \tag{2.28}$$

\vdots

$$\text{Controller } N_s \tag{2.29}$$

$$\text{Model output } N_s \tag{2.30}$$

At each time step 1 to N_s , the corresponding QDMCs are as follows:

Controller 1

$$\begin{aligned}
 & \min_{\Delta \mathbf{u}_1} \frac{1}{2} \Delta \mathbf{u}_1^T H \Delta \mathbf{u}_1 + \mathbf{g}_1^T \Delta \mathbf{u}_1 \\
 & \text{s.t.} \quad I_L \Delta \mathbf{u}_1 \leq \mathbf{u}_{max} - \mathbf{u}_0 - \mathbf{u}_{ss} \\
 & \quad \quad -I_L \Delta \mathbf{u}_1 \leq -\mathbf{u}_{min} + \mathbf{u}_0 + \mathbf{u}_{ss} \\
 & \quad \quad \mathbf{g}_1 = A^T \Gamma^T \Gamma (\mathbf{y}_1^* + \hat{\mathbf{d}}_1 - \mathbf{y}_{sp})
 \end{aligned} \tag{2.31}$$

Model output 1

$$\begin{aligned}\hat{y}_1 &= y_{1|1}^* + \hat{d}_1 + y_{sp} \\ y_{min} &\leq \hat{y}_1 \leq y_{max}\end{aligned}$$

In the above,

$$\mathbf{u}_o = u_o \mathbf{e} \quad (2.32)$$

$$\mathbf{u}_{ss} = u_{ss} \mathbf{e} \quad (2.33)$$

Controller 2

$$\begin{aligned}\min_{\Delta \mathbf{u}_2} & \frac{1}{2} \Delta \mathbf{u}_2^T H \Delta \mathbf{u}_2 + \mathbf{g}_2^T \Delta \mathbf{u}_2 \\ \text{s.t.} & \quad I_L \Delta \mathbf{u}_2 \leq \mathbf{u}_{max} - \mathbf{u}_1 - \mathbf{u}_{ss} \\ & \quad -I_L \Delta \mathbf{u}_2 \leq -\mathbf{u}_{min} + \mathbf{u}_1 + \mathbf{u}_{ss} \\ & \quad \mathbf{g}_2 = A^T \Gamma^T \Gamma (\mathbf{y}_2^* + \hat{\mathbf{d}}_2 - \mathbf{y}_{sp})\end{aligned} \quad (2.34)$$

Model output 2

$$\begin{aligned}\hat{y}_2 &= y_{2|2}^* + \hat{d}_2 + y_{sp} \\ y_{min} &\leq \hat{y}_2 \leq y_{max} \\ &\vdots\end{aligned} \quad (2.35)$$

Controller N_s

$$\begin{aligned}\min_{\Delta \mathbf{u}_{N_s}} & \frac{1}{2} \Delta \mathbf{u}_{N_s}^T H \Delta \mathbf{u}_{N_s} + \mathbf{g}_{N_s}^T \Delta \mathbf{u}_{N_s} \\ \text{s.t.} & \quad I_L \Delta \mathbf{u}_{N_s} \leq \mathbf{u}_{max} - \mathbf{u}_{N_s-1} - \mathbf{u}_{ss} \\ & \quad -I_L \Delta \mathbf{u}_{N_s} \leq -\mathbf{u}_{min} + \mathbf{u}_{N_s-1} + \mathbf{u}_{ss} \\ & \quad \mathbf{g}_{N_s} = A^T \Gamma^T \Gamma (\mathbf{y}_{N_s}^* + \hat{\mathbf{d}}_{N_s} - \mathbf{y}_{sp})\end{aligned} \quad (2.36)$$

Model output N_s

$$\begin{aligned}\hat{y}_{N_s} &= y_{N_s|N_s}^* + \hat{d}_{N_s} + y_{sp} \\ y_{min} &\leq \hat{y}_{N_s} \leq y_{max}\end{aligned}\quad (2.37)$$

Nature of interaction between the master problem and the subproblems

In this section, the nature of interaction between the master problem (the optimization problem of the decision making at level 1) and the subproblems (the optimization problem of the decision making at levels 2,3,...) as shown in Figure 2.4 will be discussed.

When the master decision variable is set at a particular level, it influences the subproblem in two ways, through the constraints:

1. Through u_{ss} term.

$$I_L \Delta \mathbf{u}_k \leq \mathbf{u}_{max} - \mathbf{u}_{k-1} - \mathbf{u}_{ss} \quad (2.38)$$

$$-I_L \Delta \mathbf{u}_k \leq -\mathbf{u}_{min} + \mathbf{u}_{k-1} + \mathbf{u}_{ss} \quad (2.39)$$

$$u_{ss} = y_{sp} + b \quad (2.40)$$

2. And also through the objective function in its g_k

When the subproblems are optimized, the master problem may be required to change the variables because the new values for the subproblem's variables may turn the constraints of the master problem infeasible. This formulation allows feedback to the master problem, which in turn uses it in the search for the optimal settings for the decision variables. Therefore, a two-way interaction pattern is established and it will terminate in either an optimal or infeasible solution for master and/or subproblems.

Solution Algorithm

The inner problems will be replaced by their Karush–Kuhn–Tucker conditions. This converts the above problem into single-level optimization problem with λ , the lagrange mul-

multipliers for the problem, as additional problem variables.

This method replaces the subproblems by the Karush–Kuhn–Tucker conditions, and then transforms the multi-level problem into a mixed-integer quadratic programming problem by exploiting the disjunctive nature of the complementarity slackness conditions where binary variables are used to choose the binding constraints for the inner problem. This approach allows the control of all variables to be given to the leader (the master problem) so we will essentially be dealing with a one level program. Fortuny-Amat and McCarl [1981] developed an approach to find the global optimum of the bilevel optimization problem, however the approach is not the most efficient way to solve the multilevel optimization problems.

The formulation provides as follows:

$$\min_{\Delta \mathbf{u}_k} \frac{1}{2} \Delta \mathbf{u}_k^T H \Delta \mathbf{u}_k + \mathbf{g}_k^T \Delta \mathbf{u}_k \quad (2.41)$$

$$s.t \quad I_L \Delta \mathbf{u}_k - \mathbf{u}_{max} + \mathbf{u}_{k-1} + \mathbf{u}_{ss} \leq 0 \quad (2.42)$$

$$- I_L \Delta \mathbf{u}_k + \mathbf{u}_{min} - \mathbf{u}_{k-1} - \mathbf{u}_{ss} \leq 0 \quad (2.43)$$

The optimization subproblems are replaced by its KKT conditions and then the slack variables are added to the constraints 2.42 and 2.43 as follows:

$$\begin{aligned} \mathcal{L}(\Delta \mathbf{u}_k, \lambda_1, \lambda_2) = & \frac{1}{2} \Delta \mathbf{u}_k^T H \Delta \mathbf{u}_k + \mathbf{g}_k^T \Delta \mathbf{u}_k \\ & + \lambda_1^T (I_L \Delta \mathbf{u}_k - \mathbf{u}_{max} + \mathbf{u}_{k-1} + \mathbf{u}_{ss}) \\ & + \lambda_2^T (-I_L \Delta \mathbf{u}_k + \mathbf{u}_{min} - \mathbf{u}_{k-1} - \mathbf{u}_{ss}) \end{aligned} \quad (2.44)$$

The KKT conditions then become

$$\frac{\partial \mathcal{L}(\Delta \mathbf{u}_k, \lambda_1, \lambda_2)}{\partial \Delta \mathbf{u}_k^T} = 0 = H \Delta \mathbf{u}_k + \mathbf{g}_k + I_L^T \lambda_1 - I_L^T \lambda_2 \quad (2.45)$$

$$0 = I_L \Delta \mathbf{u}_k + \mathbf{u}_{k-1} + \mathbf{u}_{ss} - \mathbf{u}_{max} + \mathbf{v}_1 \quad (2.46)$$

$$0 = -I_L \Delta \mathbf{u}_k - \mathbf{u}_{k-1} - \mathbf{u}_{ss} + \mathbf{u}_{min} + \mathbf{v}_2 \quad (2.47)$$

$$0 = \lambda_1^T \mathbf{v}_1 \quad (2.48)$$

$$0 = \lambda_2^T \mathbf{v}_2 \quad (2.49)$$

$$\lambda_1, \lambda_2, \mathbf{v}_1, \mathbf{v}_2 > 0 \quad (2.50)$$

where

λ_1 : is a vector that represents the Lagrange multipliers for the upper bound of the manipulated variables

λ_2 : is a vector that represents the lagrange multipliers for the lower bound of manipulated variable

\mathbf{v}_1 : is a vector that represents the nonnegative slack variables of the constraint

\mathbf{v}_2 : is a vector that represents the nonnegative slack variables of the constraint

This transformed problem described in equation 2.45 to 2.50 is a nonlinear, nondifferentiable and nonconvex problem and cannot be easily solved by using standard nonlinear programming [Bard and Moore, 1990].

Complementarity conditions

The complementarity condition constraints are one of the major difficulties in solving the transformed single-level problem. They involve discrete decisions on the choice of active set constraints of the inner problem. The active set changes when at least one inequality function and its multiplier are equal to zero. With the change in the active set of constraints, the overall feasible space changes. In order to overcome these difficulties, Fortuny-Amat and McCarl [1981] suggested suppressing the complementarity conditions $\lambda^T v = 0$ by introducing the binary variables \mathbf{z}_1 and \mathbf{z}_2 and solving the resulting linear Equation (2.51) instead. Hence, the complementarity conditions can be formulated as follows:

$$\begin{aligned}
0 &\leq \lambda_1 \leq z_1 B \\
0 &\leq \lambda_2 \leq z_2 B \\
0 &\leq \mathbf{v}_1 \leq (1 - z_1)B \\
0 &\leq \mathbf{v}_2 \leq (1 - z_2)B
\end{aligned} \tag{2.51}$$

where B is an upper bound for the slack variables \mathbf{v}_1 and \mathbf{v}_2 .

Hence, we can combine the equations 2.45 to 2.51 as following:

$$0 = H\Delta\mathbf{u}_k + \mathbf{g}_k + I_L^T \lambda_1 - I_L^T \lambda_2 \tag{2.52}$$

$$0 \leq -I_L \Delta\mathbf{u}_k - \mathbf{u}_{k-1} - \mathbf{u}_{ss} + \mathbf{u}_{max} \leq (1 - z_1)B \tag{2.53}$$

$$0 \leq +I_L \Delta\mathbf{u}_k + \mathbf{u}_{k-1} + \mathbf{u}_{ss} - \mathbf{u}_{min} \leq (1 - z_2)B \tag{2.54}$$

$$0 \leq \lambda_1 \leq z_1 B \tag{2.55}$$

$$0 \leq \lambda_2 \leq z_2 B \tag{2.56}$$

$$\mathbf{z}_1, \mathbf{z}_2 \in \{0, 1\} \tag{2.57}$$

$$\lambda_1, \lambda_2 \geq 0 \tag{2.58}$$

and finally the one level optimization problem will be:

$$\min_{y_{sp}} (y_{sp} - y_{tgt})^2$$

$$\text{Subject to } y_{min} \leq y_{sp} \leq y_{max}$$

$$u_{ss} = a y_{sp} + b$$

$$H = A_T \Gamma^T \Gamma A + \Lambda^T \Lambda$$

Controller and model output 1

$$0 = H \Delta \mathbf{u}_1 + \mathbf{g}_1 + I_L^T \lambda_1^1 - I_L^T \lambda_2^1$$

$$0 \leq -I_L \Delta \mathbf{u}_1 - \mathbf{u}_o - \mathbf{u}_{ss} + \mathbf{u}_{max} \leq (1 - \mathbf{z}_1^1) B$$

$$0 \leq +I_L \Delta \mathbf{u}_1 + \mathbf{u}_o + \mathbf{u}_{ss} - \mathbf{u}_{min} \leq (1 - \mathbf{z}_2^1) B$$

$$0 \leq \lambda_1^1 \leq \mathbf{z}_1^1 B$$

$$0 \leq \lambda_2^1 \leq \mathbf{z}_2^1 B$$

$$\hat{y}_1 = y_{1|1}^* + \hat{d}_1 + y_{sp}$$

$$y_{min} \leq \hat{y}_1 \leq y_{max}$$

$$\mathbf{z}_1^1, \mathbf{z}_2^1 \in \{0, 1\}, \quad \lambda_1^1, \lambda_2^1 \geq 0$$

Controller and model output 2

$$0 = H \Delta \mathbf{u}_2 + \mathbf{g}_2 + I_L^T \lambda_1^2 - I_L^T \lambda_2^2$$

$$0 \leq -I_L \Delta \mathbf{u}_2 - \mathbf{u}_1 - \mathbf{u}_{ss} + \mathbf{u}_{max} \leq (1 - \mathbf{z}_1^2) B$$

$$0 \leq +I_L \Delta \mathbf{u}_2 + \mathbf{u}_1 + \mathbf{u}_{ss} - \mathbf{u}_{min} \leq (1 - \mathbf{z}_2^2) B$$

$$0 \leq \lambda_1^2 \leq \mathbf{z}_1^2 B$$

$$0 \leq \lambda_2^2 \leq \mathbf{z}_2^2 B$$

$$\hat{y}_2 = y_{2|2}^* + \hat{d}_2 + y_{sp}$$

$$y_{min} \leq \hat{y}_2 \leq y_{max}$$

$$\mathbf{z}_1^2, \mathbf{z}_2^2 \in \{0, 1\}, \quad \lambda_1^2, \lambda_2^2 \geq 0$$

\vdots

$$\vdots$$

Controller and model output $\ell = N_s$

$$0 = H\Delta\mathbf{u}_{N_s} + \mathbf{g}_{N_s} + I_L^T \lambda_1^{N_s} - I_L^T \lambda_2^{N_s}$$

$$0 \leq -I_L \Delta\mathbf{u}_{N_s} - \mathbf{u}_{N_s-1} - \mathbf{u}_{ss} + \mathbf{u}_{max} \leq (1 - \mathbf{z}_1^{N_s})B$$

$$0 \leq +I_L \Delta\mathbf{u}_{N_s} + \mathbf{u}_{N_s-1} + \mathbf{u}_{ss} - \mathbf{u}_{min} \leq (1 - \mathbf{z}_2^{N_s})B$$

$$0 \leq \lambda_1^{N_s} \leq \mathbf{z}_1^{N_s} B$$

$$0 \leq \lambda_2^{N_s} \leq \mathbf{z}_2^{N_s} B$$

$$\hat{y}_{N_s} = y_{N_s|N_s}^* + \hat{d}_{N_s} + y_{sp}$$

$$y_{min} \leq \hat{y}_{N_s} \leq y_{max}$$

$$\mathbf{z}_1^{N_s}, \mathbf{z}_2^{N_s} \in \{0, 1\}, \quad \lambda_1^{N_s}, \lambda_2^{N_s} \geq 0$$

2.4 Software

The methods used to solve pure integer and mixed integer programming problems require dramatically more mathematical computation than those for similarly sized pure linear programs. Gams provides solvers for mixed integer nonlinear programming (MINLP), and solvers for mixed integer quadratic programming (MIQP) was introduced in the latest version of Gams. A brief introduction to Dicopt and SBB as examples of MINLP solvers and Cplex as an example of MIQP solvers will be discussed. All of the simulation work for this chapter has been done using MINLP solvers before MIQP availability in Gams latest edition(Sep.2004)

DICOPT

DICOPT (DIscrete and Continuous OPTimizer) is a program for solving mixed-integer nonlinear programming (MINLP) problems that involve linear binary or integer variables and linear and nonlinear continuous variables. While the modeling and solution of these MINLP optimization problems has not yet reached the stage of maturity and reliability

as linear, integer or non-linear programming modeling, these problems have a rich area of applications. For example, they often arise in engineering design, management sciences, and finance. The program is based on the extensions of the outer-approximation algorithm for the equality relaxation strategy. The MINLP algorithm inside DICOPT solves a series of NLP and MIP subproblems. These sub-problems can be solved using any NLP (Non-linear Programming) or MIP (Mixed-Integer Programming) solver that runs under GAMS. Although the algorithm has provisions to handle non-convexities, it does not necessarily obtain the global optimum [Grossmann *et al.*, 2004].

SBB

SBB is a relatively new GAMS solver for Mixed Integer Nonlinear Programming (MINLP) models. It is based on a combination of the standard Branch and Bound method known from Mixed Integer Linear Programming and some of the standard NLP solvers already supported by GAMS.

Cplex

GAMS/Cplex is a GAMS solver that allows users to combine the high level modelling capabilities of GAMS with the power of Cplex optimizers. Cplex optimizers are designed to solve large, difficult problems quickly and with minimal user intervention. Cplex solution algorithms include linear, quadratically constrained and mixed integer programming problems. While numerous solving options are available, GAMS/Cplex automatically calculates and sets most options at the best values for specific problems.

For problems with integer variables, Cplex uses a branch and cut algorithm which solves a series of LP, subproblems. Because a single mixed integer problem generates many subproblems, even small mixed integer problems can be very computationally intensive and require significant amounts of physical memory. Cplex can also solve problems of GAMS model type Mixed Integer Quadratic Constrained Programming (MIQCP). As in the continuous case, if the base model is a QP the Simplex methods can be used and duals will be available at the solution. If the base model is a QCP, only the Barrier method can be used for the nodes and only primal values will be available at the solution [GAMS, 1998].

Computer Ssystem

Computer system used: laptop, Pentium 4 with processor 2.4. 1024 MB cash memory.

2.5 Case Studies

2.5.1 Isothermal CSTR

This single–input single–output continuous stirred tank isothermal reactor model is taken, in part, from the work of Marlin [2000]. The objective of this case study is to find the optimum back–off from constraints using constrained MPC as the controller.

Process description and specification

In this section the transfer function model, together with simplifying assumptions will be outlined. Controlled and manipulated variables, a description of the constraints and disturbance will be outlined.

Process model and objective function

The system is illustrated in Figure 2.5 with the steady–state and dynamic model below.

An isothermal first order reaction $A \rightarrow B$ takes place in the liquid phase. It is desired to produce B within specification. The process model consists of one transfer function model that describes the change in the outlet concentration.

Process transfer function model Controlled variable: outlet concentration from the reactor C_A (mole/m³) Manipulated variable: inlet feed flow rate F (m³/min)

$$C'_A(s) = \frac{2.722}{12.4s + 1} F'(s) \quad (2.59)$$

where the prime indicates a deviation from the steady–state.

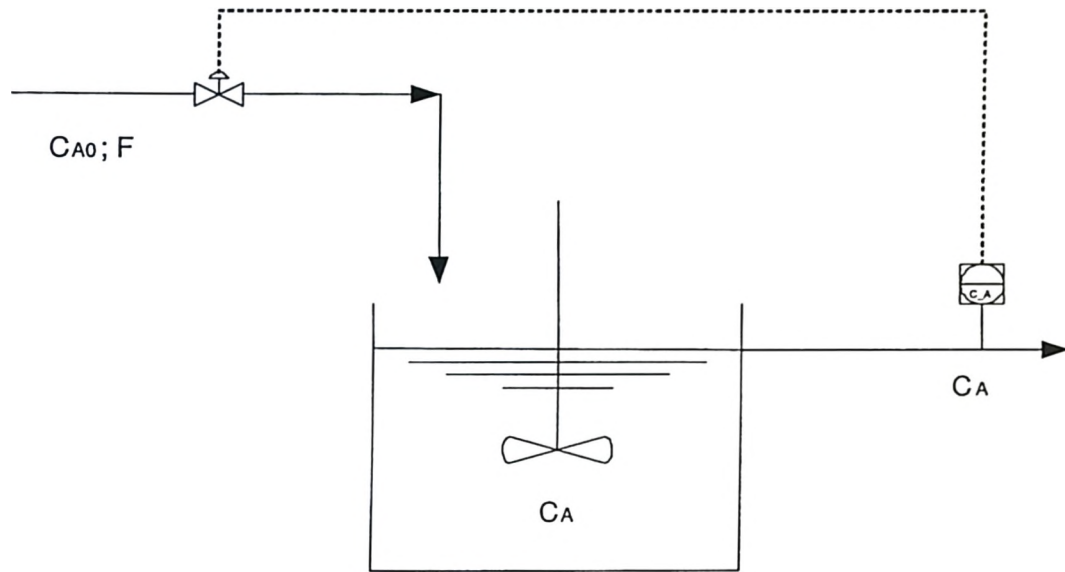


Figure 2.5: Continuous stirred tank reactor(CSTR)

Disturbance model

A step change in the inlet concentration will be considered as disturbance. The disturbance time constant is assumed to 7 min.

$$C'_A(s) = \frac{0.503}{12.4s + 1} C'_{A0}(s) \quad (2.60)$$

Dynamic Model

$$V \frac{dC_A}{dt} = F(C_{A0} - C_A) - V k C_A \quad (2.61)$$

Steady-state linear Model

$$C_{A_{ss}} - \bar{C}_{A_{ss}} = 2.722(F_{ss} - \bar{F}_{ss}) + 0.503\Delta d \quad (2.62)$$

Constraints

$$0.50 \leq C_A \leq 0.85 \text{ mole/m}^3 \quad (2.63)$$

$$0.05 \leq F \leq 0.90 \text{ m}^3/\text{min} \quad (2.64)$$

Target set-point

The target set-point was chosen to be 0.85 mole/m³

Model predictive control

The tuning parameters (which are the objective function weighting matrices), the output prediction horizon and input control moves are selected and assumed constant as described in the Table 2.3. A sampling time of 3 minutes was used and the simulation horizon chosen to be 90 minutes.

parameters	Description	Value
M	Control move horizon	2
P	Prediction horizon	10
N_S	Simulation horizon	31
Γ	Controlled variables weighting	I
Λ	Manipulated variables weighting	I

Table 2.1: MPC tuning parameters

Simulation results

Cplex is used for simulating the isothermal CSTR. Table (2.2) shows the number of continuous variables, integer variables, number of iterations and CPU time used for case 3.

Solvers	MINLP		MIQCP		
	SBB	Dicopt	Cplex	SBB	Baron
Solution	-	0.0045	0.0045	-	0.0045
Number of variables	1646	1646	1646	1646	1646
Number of Integer variables	124	124	124	124	124
CPU time used	>4 hrs	112 sec	1.03 sec	> 4 hrs	954 sec

Table 2.2: Comparison of the different solvers

1- Manipulated variable is not saturated

Step change in inlet concentration = 0.1 mole/m^3

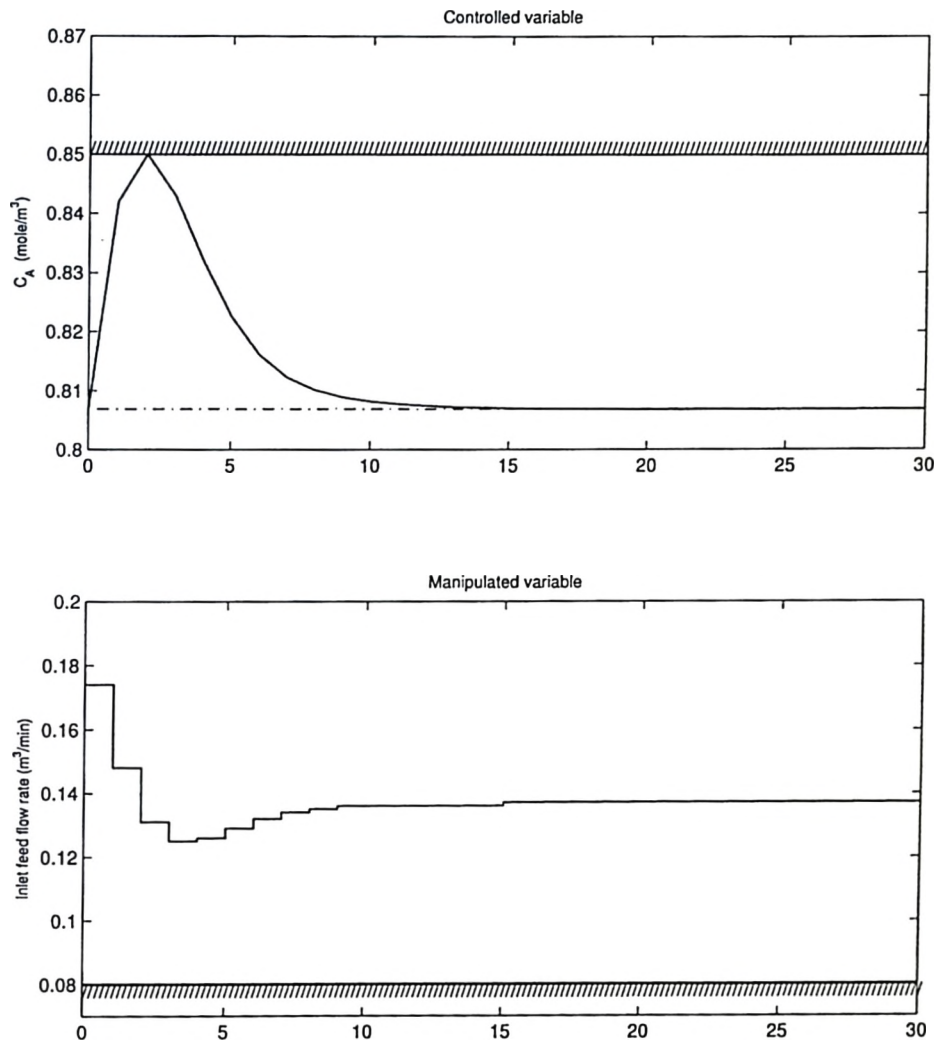


Figure 2.6: Manipulated variable is not saturated

In Figure 2.6, the set-point is backed-off from the constraints from 0.85 to 0.807 mole/m^3 .

2- Manipulated variable touching the constraints without saturation

Step change in inlet concentration = 0.29 mole/m^3

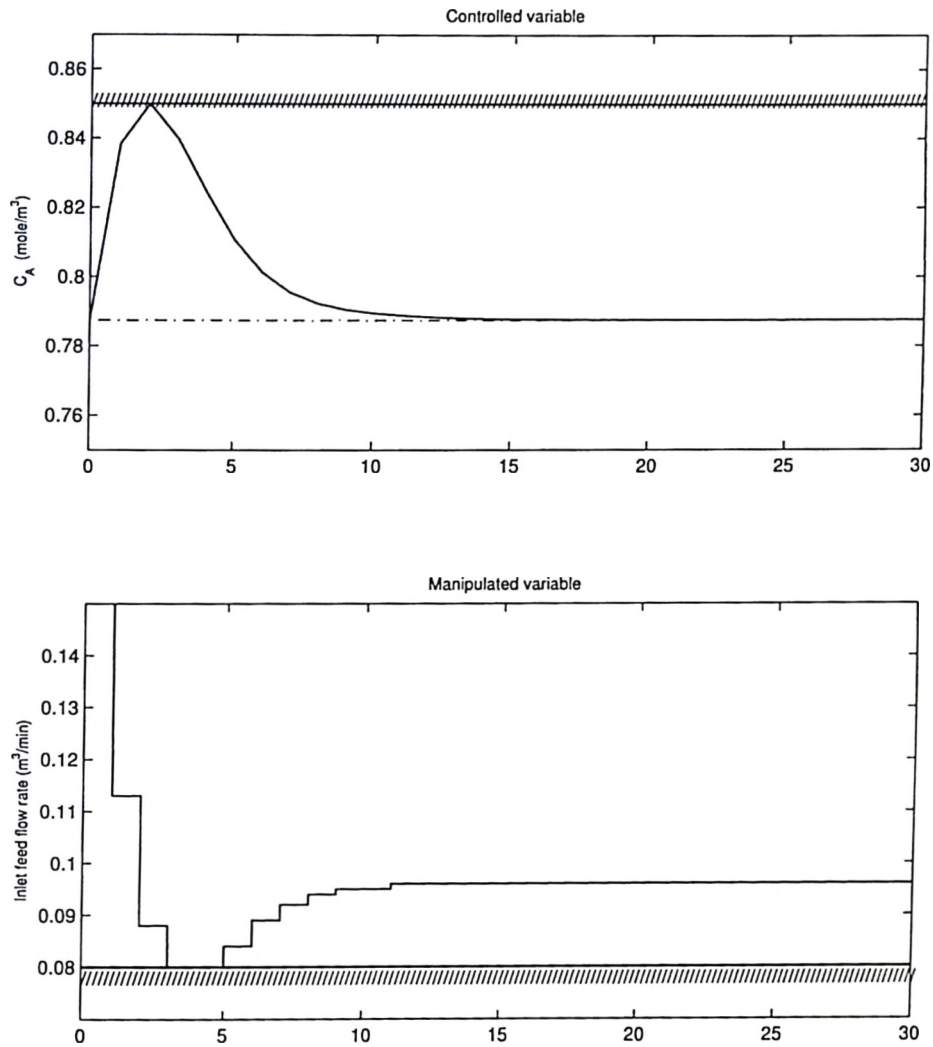


Figure 2.7: Manipulated variable is touching the lower bound without saturation

In Figure 2.7, the set-point is backed-off from the constraints from 0.85 to 0.79 mole/m^3 .

3- Manipulated variable partially saturated

Step change in inlet concentration = 0.31 mole/m^3

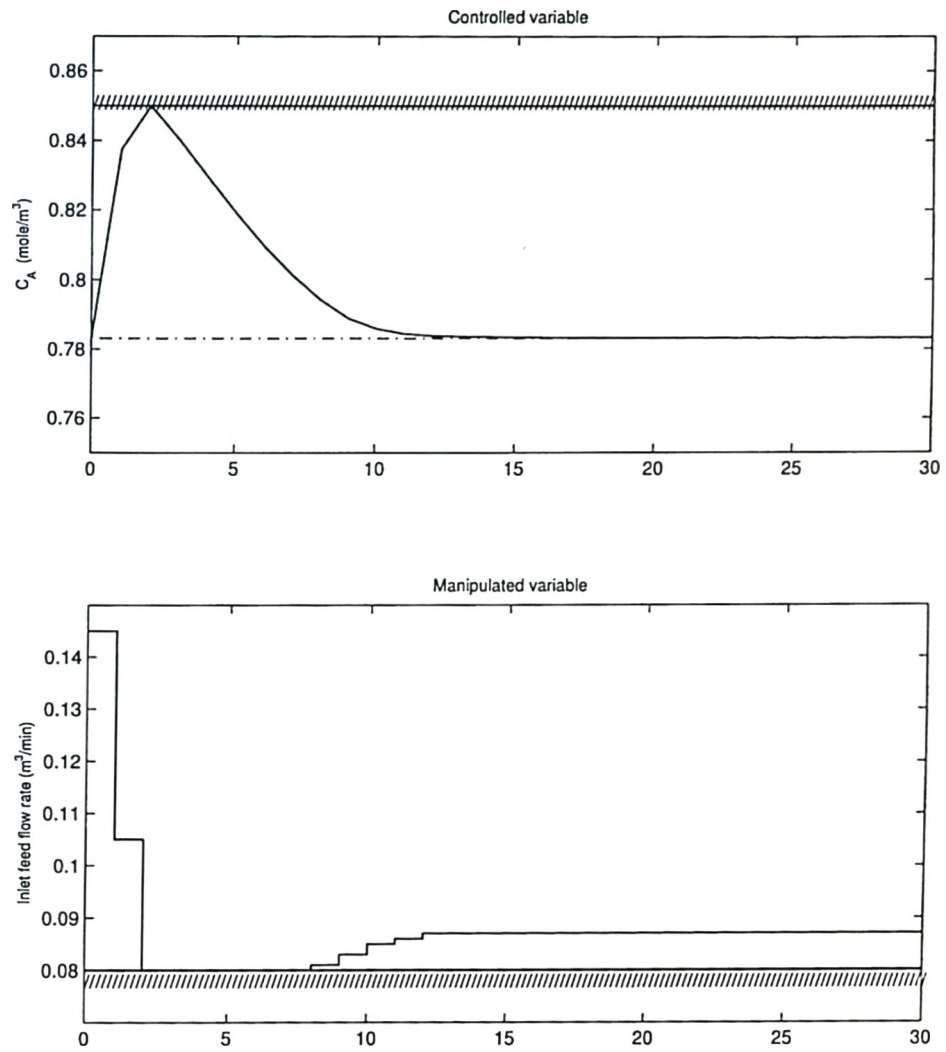


Figure 2.8: Manipulated variable is partially saturated

4- Manipulated variable is saturated

Step change in inlet concentration = 0.327 mole/m^3

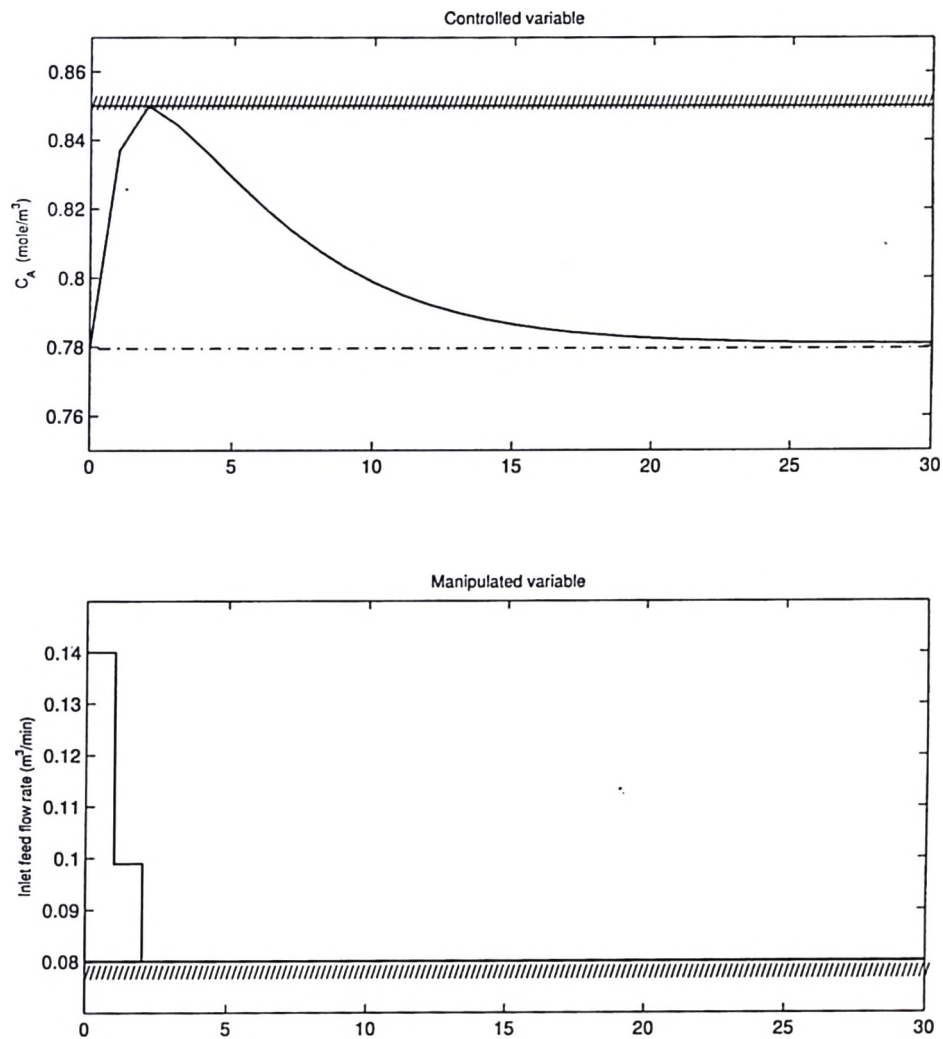


Figure 2.9: Manipulated variable is completely saturated

In Figure 2.9, the set-point is backed-off from the constraints from 0.85 to 0.78 mole/m³. The manipulated variable is completely saturated

2.5.2 Fluid catalytic cracking unit (FCCU)

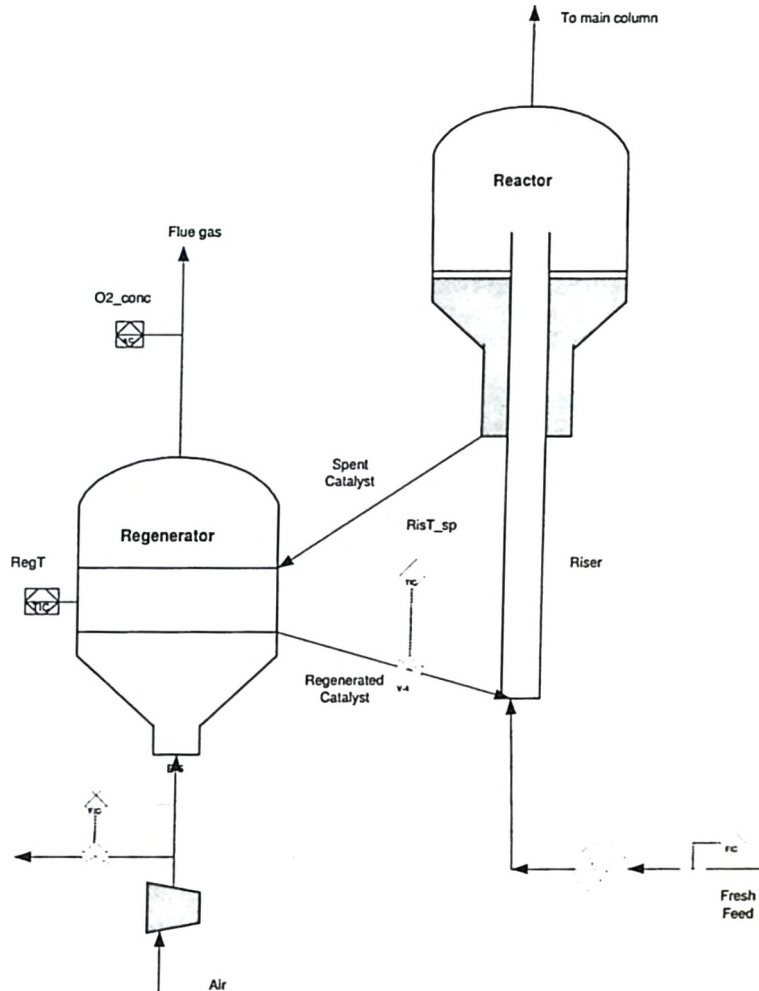


Figure 2.10: Fluid catalytic cracking unit (FCCU)

Process description and specification

The fluid catalytic cracking (FCC) unit is one of the most important and complicated processes in the petroleum refining industry. The complexity of the process, from both the modeling and control points of view, arises from the strong interactions between the two reactors, namely the riser reactor and the regenerator reactor. An FCCU converts gas oil

into a range of hydrocarbon products of which gasoline is the most valuable. The amount of low market-value feedstocks available for catalytic cracking is considerable for any refinery. The ability of a typical FCC unit to produce gasoline from low market value feedstocks gives the FCC a major role in overall economic performance of the refinery. Operating the FCC unit at or close to the optimum will have a considerable effect on the overall economic performance of the refinery. Therefore it is a prime candidate for any study of interaction between RTO and control.

Process model: The original work of Ansari and Tad [2000] identified a 5-input 4-output linear transfer function model for fluid catalytic cracking unit (FCCU) model by making step changes in the manipulated variables. Here a subset of the of the their model was selected to conduct this study.

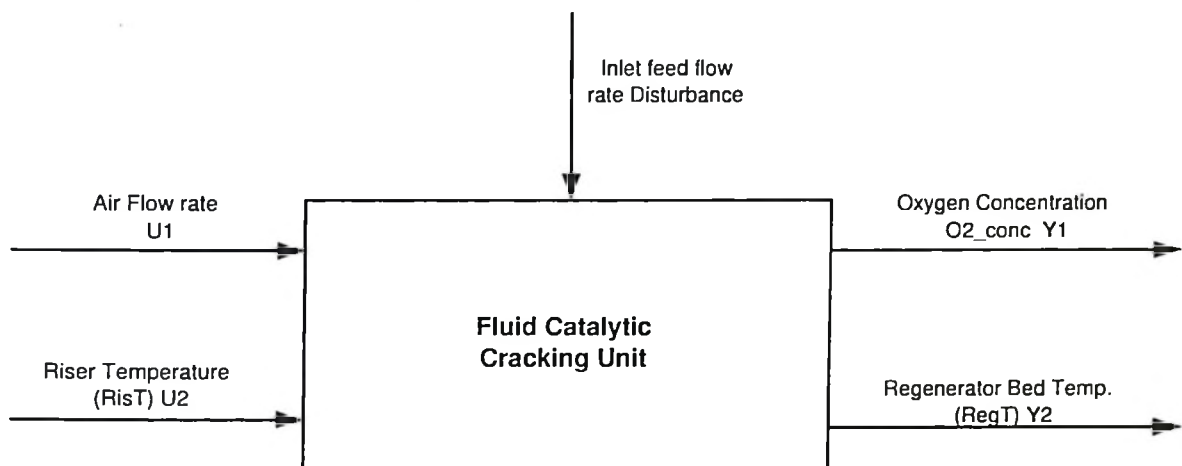


Figure 2.11: Schematic of model predictive control problem for the catalytic cracking reactor-regenerator system

Controlled variables (Cvs)

$y_1(s)$	Oxygen concentration in the outlet flue gases from the regenerator	[vol%]
$y_2(s)$	Regenerator bed temperature	[C°]

Manipulated variables (Mvs)

$u_1(s)$	Inlet air flow rate to the regenerator	[ton/hr]
$u_2(s)$	Riser outlet temperature	[C°]

Disturbance

$d(s)$	Inlet feed flow rate	[m ³ /hr]
--------	----------------------	----------------------

Process model

$$\begin{bmatrix} y_1(s) \\ y_2(s) \end{bmatrix} = \begin{bmatrix} \frac{0.10(1.7s+1)e^{-2s}}{18s^2+7s+1} & \frac{-0.080(4.8s+1)}{9s^2+3s+1} \\ \frac{0.08e^{-4s}}{11s^2+8s+1} & \frac{0.8(1.7s+1)e^{-2s}}{10s^2+7.3s+1} \end{bmatrix} \begin{bmatrix} u_1(s) \\ u_2(s) \end{bmatrix} + \begin{bmatrix} \frac{-0.90e^{-2s}}{13s^2+4.6s+1} \\ \frac{0.45e^{-4s}}{23s^2+8s+1} \end{bmatrix} d(s) \quad (2.65)$$

where all variables are in deviation form and units in square brackets:

Constraints: The operating variables constraints were not available in the original work, so model constraints limits based on Grosdidier *et al.* [1993] are used instead:

$$0.7 \leq y_1(s) \leq 1.3 \text{ [vol\%]}$$

$$705 \leq y_2(s) \leq 735 \text{ [C}^\circ\text{]}$$

$$140 \leq u_1(s) \leq 155 \text{ [ton/hr]}$$

$$515 \leq u_2(s) \leq 535 \text{ [C}^\circ\text{]}$$

Steady-state relation ship between the inputs and the outputs

$$\begin{bmatrix} y_{ss1} - \bar{y}_{ss1} \\ y_{ss2} - \bar{y}_{ss2} \end{bmatrix} = \begin{bmatrix} 0.10 & -0.080 \\ 0.08 & 0.8 \end{bmatrix} \begin{bmatrix} u_{ss1} - \bar{u}_{ss1} \\ u_{ss2} - \bar{u}_{ss2} \end{bmatrix} + \begin{bmatrix} -0.90 \\ 0.45 \end{bmatrix} \Delta d \quad (2.66)$$

where:

- y_{ss1} : Steady-state oxygen concentration in the outlet flue gases from the regenerator [vol%]
- y_{ss2} : Steady-state regenerator bed temperature [C°]
- u_{ss1} : Steady-state inlet air flow rate to the regenerator [ton/hr]
- u_{ss2} : Steady-state riser outlet temperature [C°]
- \bar{y} : Refers to the initial output steady-state
- \bar{u} : Refers to the initial input steady-state

Target set-point

Target set-point for oxygen concentration was chosen to be 0.7 Vol%, while the set-point for regenerator temperature was 705C°

Model predictive control

The output prediction horizon and control move horizon are selected and assumed constant as described in the Table 2.3. A sampling time of 2 minutes was used and the simulation horizon chosen to be 50 minutes.

parameters	Description	Value
M	Control moves	2
P	Prediction horizon	10
N_S	Simulation horizon, steps	26

Table 2.3: MPC tuning parameters

Controlled variable weighting matrix

$$\Gamma = \begin{bmatrix} 1 & 0 \\ 0 & 1 \end{bmatrix} \quad (2.67)$$

Manipulated variable weighting matrix

$$\Lambda = \begin{bmatrix} 0.1 & 0 \\ 0 & 1 \end{bmatrix} \quad (2.68)$$

Simulation Results

Simulation results for small disturbances

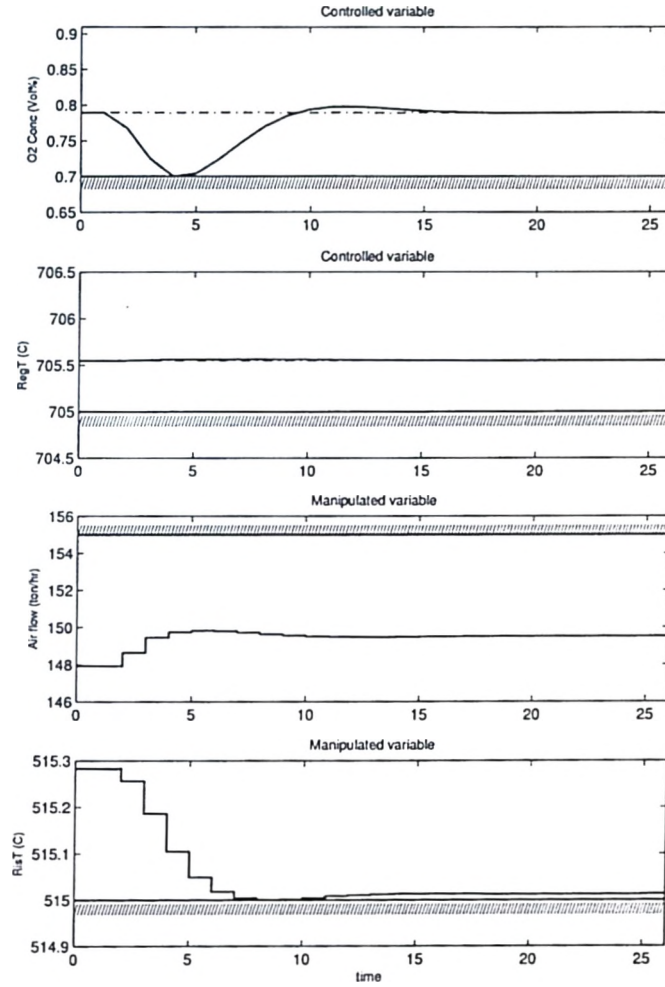


Figure 2.12: Effect of small disturbances on the manipulated and controlled variables

Fig 2.12 shows the effect of a small disturbance (step change in inlet feed flow rate = 0.2 m³/hr). u_1 is not saturated while y_1 is touching the constraints. The oxygen concentration set-point to the controller has to be backed-off from 0.7 to 0.78 vol%

Partial Saturation of the inlet air flow rate (u_1) and Riser Temperature (u_2)

Step change in inlet feed flow rate = $0.42 \text{ m}^3/\text{hr}$

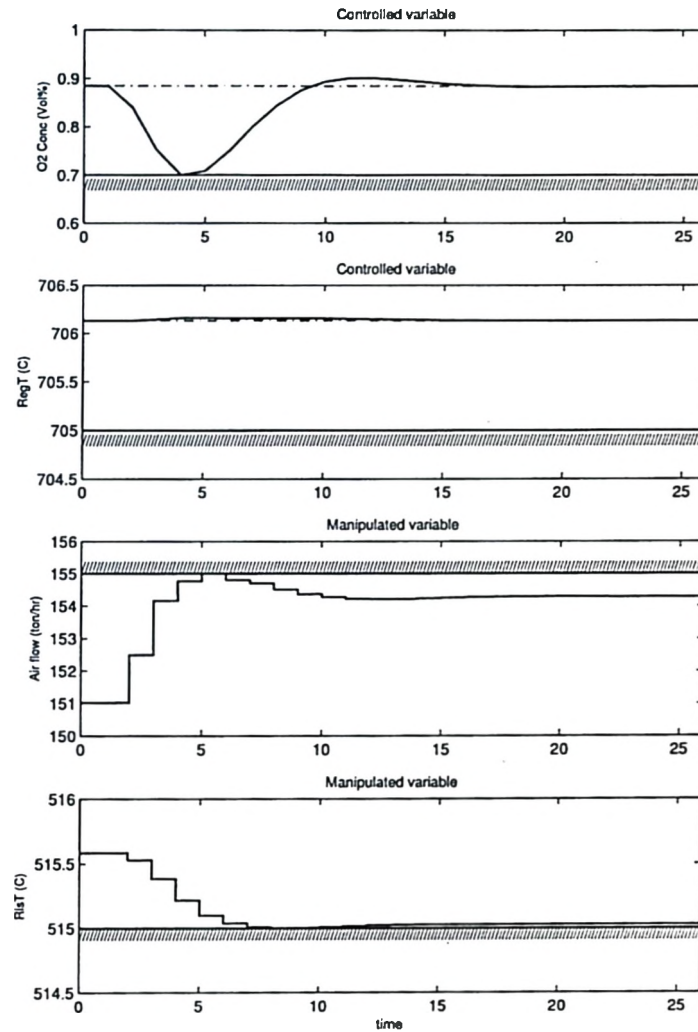


Figure 2.13: Both of the manipulated variables are partially saturated

Fig 2.13 shows the effect of a large disturbance (step change in inlet feed flow rate = $0.42 \text{ m}^3/\text{hr}$). Both of the manipulated variables u_1 and u_2 are partially saturated and the oxygen concentration set-point to the controller has to back-off from 0.7 to 0.89 vol%.

Both of the manipulated variables saturated

Step change in inlet feed flow rate = $0.47 \text{ m}^3/\text{hr}$. Lower bound on oxygen concentration=0.7

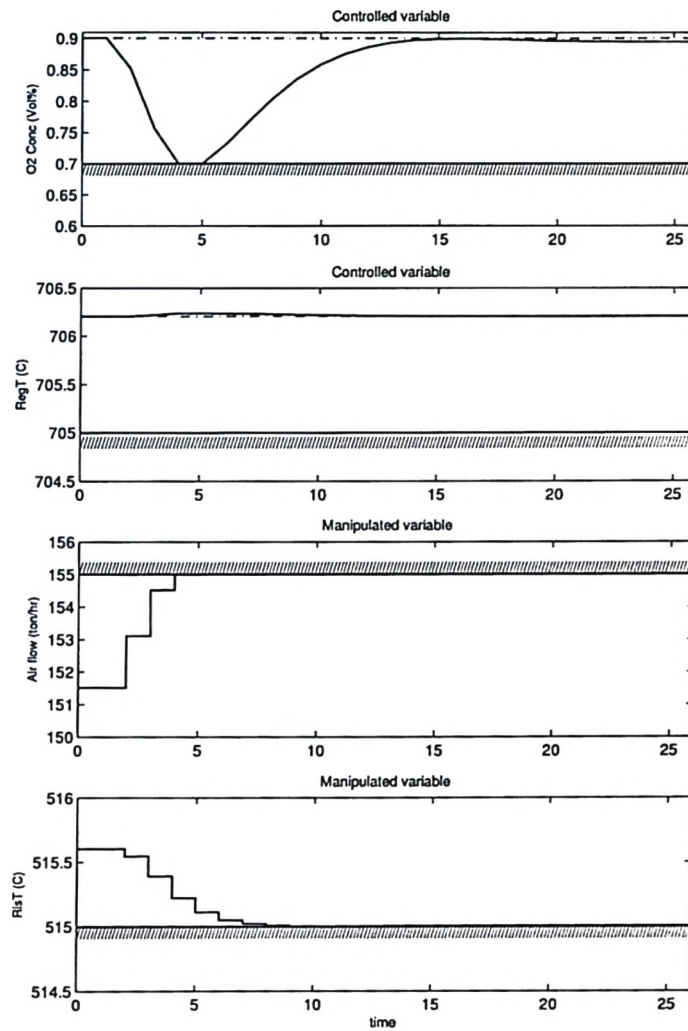


Figure 2.14: Both of the manipulated variables are saturated

Both of the manipulated variables u_1 and u_2 are saturated and the oxygen concentration set-point to the controller has to back-off from 0.7 to 0.9 vol%.

2.6 Future Work

In this study, the disturbance is assumed to be specified or estimated. Therefore this work needs to be extended to include estimation for the unmeasured disturbances.

Alternative computation strategies are required to be developed in order to handle large MIMO systems because standard algorithms are not suitable particularly when the number of the integer variables increases. An interior point approach or more efficient branch and bound strategy might be used.

Further extensions include consideration of process model mismatch and nonlinearities.

Chapter 3

Modelling of a Continuous Oxygen Delignification Unit

3.1 Introduction

Due to strict environmental regulations on the use of chlorine in pulp bleaching, many oxygen delignification reactors have been added to existing paper mills to reduce the consumption of chlorine in bleaching units. The first commercial oxygen delignification unit was introduced in South Africa in 1970. The oxygen delignification stage is carried out to the farthest extent to remove the maximum amount of lignin without carbohydrate degradation before the pulp is passed on to the chlorination reactor. Therefore, improvement in the oxygen delignification processes can have a significant impact on the economic feasibility and controllability of bleaching plants. Lignin is the glue that binds fibres in the pulp. It is a measure of the demand of potassium permanganate during oxidation of the pulp under certain standardized conditions. The use of an oxygen stage before chlorination in pulp bleaching plants can reduce the chemical oxygen demand (COD) of waste streams by 50% and the biological oxygen demand by 25-50 %. Furthermore, savings in chemical costs of more than 25% may be achieved through reducing the use of chlorine, chlorine dioxide

and hypochlorite [Hsu and Hsieh, 1988]. The dissolved material unlike that of chlorination and caustic extraction, is uncontaminated by the chloride ions so it can therefore be routed back to the recovery furnace where it becomes source of energy instead of a pollutant.

Energy related benefits include, recovery of heat from combustion of the material removed from the pulp in the oxygen stage, lower refining energy requirements of oxygen-bleached pulps and the fact that the manufacture of oxygen requires only about one-eighth of the energy needed to make a chemical equivalent of chlorine. As a result of these benefits, oxygen bleaching prior to chlorination stage has become a well-established process.

In order to benefit from the above advantages, one serious problem associated with oxygen delignification needs to be overcome. This problem arises from the natural tendency of oxygen to form reactive free radicals that can attack cellulose and other carbohydrates in addition to the lignin that is required to be broken down. This adversely affects pulp strength, and consequently poses a constraint on operation of the process.

Carbohydrate degradation is the most important factor limiting the amount of delignification that can be achieved in the oxygen stage. The success of the oxygen delignification process is dependent on its ability to overcome the selectivity problem. This can be handled by developing a nonlinear fundamental dynamic model for cellulose degradation and lignin removal. The model will allow better prediction and control of pulp properties over wide range of operating conditions. Therefore, it will be possible to run the oxygen delignification process to farthest extent of removing lignin before the chlorination process without losing the pulp strength.

This chapter describes the development of a dynamic model of an oxygen delignification unit. Its use in the development and evaluation of model-based control strategies is the subject of the next chapter. The model is based on fundamental mass and energy balances and incorporates literature-based kinetic models for prediction of the kappa number and pulp viscosity. Through the literature review, models proposed by Iribarne and Schroeder [1997] and Myers and Edwards [1989] were found to be the most suitable for many processes because they cover a wide range of operating conditions. The Myers and Edwards [1989]

model was used to describe lignin removal and the Iribarne and Schroeder [1997] model to describe the cellulose degradation. Therefore a dynamic model for the oxygen delignification reactor has been developed.

Quality variables

Kappa number: This is a quantity that gives an indirect measure of the amount of residual lignin. Kappa number is defined as the number of milliliters of 0.1 N potassium permanganate solution consumed by one gram of pulp in 10 minutes at 25 C.

According to the Casey [1980], the relation between the residual lignin in the pulp and the kappa number is :

$$L = \frac{0.147}{100} K \quad (3.1)$$

where K is the kappa number and L where [L] is the lignin mass fraction.

Pulp viscosity: Pulp viscosity is an indicator of the extent of cellulose degradation. The strength potential of the pulp is related to cellulose chain length and also to viscosity which is used as an indirect measure of pulp strength. The viscosity is determined by the average chain length of cellulose. No method is available to measure the pulp viscosity online so laboratory analysis is necessary.

Operation Variables

The most important variables affecting oxygen delignification are:

1. Caustic soda flow rate
2. Reactor temperature – The temperature in the reactor is controlled mainly by manipulating the steam flow rate.
3. Oxygen partial pressure or concentration in the liquor phase – It is desirable to keep P_{O_2} constant by manipulating the inlet oxygen flow rate.
4. Level – The reactor level is kept constant by manipulating the production rate.

3.2 Kinetic Models for Oxygen Delignification Reaction

Introduction

For optimization and control of the oxygen delignification reactor, information on its kinetics of delignification is required in order to build a dynamic model. Therefore a comparison of different kinetic models in the literature is presented here in order to come up with the most suitable overall kinetic model. This model should have the following characteristics:

1. **Reaction rate is independent of consistency:** sufficient mixing of the reactants during the experiments to avoid changing the reaction rate as the consistency varies. Myers and Edwards [1989], Hsu and Hsieh [1988] and Iribarne and Schroeder [1997] mentioned that consistency does not have an effect on the rate equation and if happened this must be due to insufficient mixing during the experiments.
2. **The model should cover wide range of operating conditions:** i.e. inlet kappa number, operating temperature, operating pressure, viscosity and consistency.
3. **High Consistency** the model should be applicable to high consistency pulp.
4. **Soft and hard wood** the model should be applicable to both soft and hard wood.

Several investigators have treated oxygen delignification kinetics such that the drop in kappa number takes place over two distinct time periods. These correspond to a rapid initial step followed by a long period over which the kappa number drops very slowly in addition to the base level.

$$K_{total} = K_f + K_s + K_{floor} \quad (3.2)$$

where

K_f : Is the amount of easily and rapidly eliminated lignin.

K_s : Is the amount of difficult and slowly eliminated lignin.

K_{floor} : Floor or final equilibrium value for kappa number (non-reacting lignin) which is approximated by 10% of the initial kappa number [Myers and Edwards, 1989].

Oxygen bleaching is a heterogeneous reaction which occurs in a system comprising of fiber(solid), water(liquid), and oxygen(gas). Two competing reactions, delignification and carbohydrate degradation, occur simultaneously during oxygen bleaching. Therefore any kinetic study of oxygen bleaching must contain the kinetics of both delignification and carbohydrate degradation.

The degree of delignification is measured by determining the kappa number of the pulp, while the carbohydrate degradation is monitored by measuring the intrinsic viscosity which can be converted to m_n , the estimated number of cellulose chains per metric ton of pulp (moles/Oven Dry metric ton (O.D.mt) of pulp).

A new chain formed means that a carbohydrate bond has been broken. The use of m_n is more suitable in kinetic studies than viscosity. This is because in kinetics, both the reactant and the products should be expressed in chemical units [Olm and Teder, 1979].

3.2.1 Olm and Teder kinetic model

Olm and Teder [1979] showed that almost all lignin in the kraft pulp can be removed with an oxygen delignification stage. However, the practical extent of delignification is limited by degradation of carbohydrates in the pulp. If allowed to proceed far enough, the degradation will result in a loss of pulp strength. This nonselectivity is currently what limits the oxygen stages to 40-50 percent delignification [Iribarne and Schroeder, 1997]

The degree of delignification is measured by determining the kappa number of the pulp, which can be described by two first order reactions with respect to the remaining lignin; an initial rapid delignification (K_f) followed by slow residual delignification (K_s).

$$-\frac{dK}{dt} = A_1 e^{\frac{-10}{RT}} [OH^-]^{0.1} P_{O_2}^{0.1} K_f + A_2 e^{\frac{-15}{RT}} [OH^-]^{0.3} P_{O_2}^{0.2} K_s \quad (3.3)$$

where

K : Is the kappa number.

K_f : Is the amount of easily and rapid eliminated lignin.

K_s : Is the amount of difficult and slowly eliminated lignin.

Carbohydrate degradation: The carbohydrate degradation is monitored by measuring the intrinsic viscosity which can be converted to m_n estimated number of cellulose chains per metric ton of pulp. m_n can be described by two zero order reactions with respect to the residual carbohydrate; an initial rapid degradation followed by slow residual degradation. For cellulose degradation

$$-\frac{dm_n}{dt} = A_{c1}e^{\frac{-40}{RT}}[OH^-]^{0.2}P_{O_2}^{0.8} + A_{c2}e^{\frac{-53}{RT}}[OH^-]^{0.6}P_{O_2}^{0.1} \quad (3.4)$$

where: m_n = number of cellulose chains per ton of pulp

Viscosity calculation:

$$\log m_n = 4.35 - 1.25 \log \eta \quad (3.5)$$

where: η = viscosity, dm^3/kg

Effect of process variables:

The delignification rate and carbohydrate degradation rate during oxygen bleaching increase with increasing the following variables :

1. Alkali concentration.
2. Oxygen partial pressure.
3. Operating temperature.
4. Consistency.

Olm and Teder [1979] indicated in their experiments that pulp consistency will affect the delignification rate and carbohydrate degradation rate in the initial phase of oxygen bleaching. However, this contradicts the conclusions of Myers and Edwards [1989], Hsu and Hsieh [1988] and Iribarne and Schroeder [1997].

Myers and Edwards [1989] mentioned that the data that Olm and Teder [1979] used did not eliminate the mixing effects. Insufficient mixing will lead to changing the reaction rate with changing the consistency. Also the model could not handle variations in the initial kappa number if it is not held constant at a value of 29.5.

We could not therefore use this model because of the following:

1. The frequency factors A_1 , A_2 , A_{c1} and A_{c2} are not provided.
2. The model could not be relied upon for inlet kappa numbers different from 29.5.
3. Consistency is affecting the initial phase delignification and carbohydrate degradation rate.

3.2.2 Hsu and Hsieh kinetic model

Hsu and Hsieh [1988] managed to remove the effect of consistency on the kappa number by running their experiments at ultra low consistency. They obtained the reaction kinetics by using the data at 0.4% consistency. They presented a two stage kinetic model to describe oxygen delignification kinetics Equation 3.6.

$$-\frac{dK}{dt} = 2.46e^{\frac{-3.6 \times 10^7}{RT}} [OH^-]^{0.78} P_{O_2}^{0.35} K^{3.07} [u(t) - u(t-2)] + 143.49e^{\frac{-7.1 \times 10^7}{RT}} [OH^-]^{0.7} P_{O_2}^{0.74} K^{3.07} [u(t-2)] \quad (3.6)$$

where:

$[OH^-]$: is the alkali concentration on solution (kmol/m³)

P_{O_2} : is the oxygen Partial pressure (N/m²)

$u(t)$ is the unit step function used to show that in the first two minutes of reaction time, the kinetic equation was described by the first term and during the remainder of the reaction time was described by the second term.

This model works for low consistency ranging from 0.4 to 4 percent so there is no effect of changing the consistency which is contradictory to Olm and Teder [1979]. The model works also for high feed kappa number 29.5.

This kinetic model fits some experimental data well, but if the initial kappa number is raised slightly the reaction rate increases too much (i.e. third order power). Hsu and Hsieh used only one initial kappa number in their experiments [Myers and Edwards, 1989].

This model is unsuitable because it is applicable to a narrow consistency(0.4-4 %) range and also for very narrow range for inlet kappa number (around 29.5).

3.2.3 Myers and Edwards kinetic model

The predictive oxygen delignification kinetic model is used for both of softwood and hardwood kraft pulps. It can also be used for all consistencies up to 30% pulps and an initial kappa number range varying from 11 to 128.

Myers and Edwards' [1989] model mainly depends on fitting data from literature that has efficient mixing and thereby, avoids dependency of the delignification rate on the consistency; It is assumed that the delignification rate is not affected at all by consistency.

They also used dissolved oxygen concentration instead of oxygen partial pressure since oxygen solubility depends on temperature as well as pressure. They did not take the effect of caustic soda on oxygen concentration into consideration. And also, they used a nonlinear caustic consumption model.

$$-\frac{dK_f}{dt} = 1.51 \times 10^5 e^{\frac{-31.6}{RT}} [O_2]^{0.43} K_f \quad (3.7)$$

$$-\frac{dK_s}{dt} = 1.68 \times 10^7 e^{\frac{-61.4}{RT}} [OH^-]^{0.875} [O_2]^{0.43} K_s \quad (3.8)$$

$$K = K_f + K_s + K_{floor} \quad (3.9)$$

The initial condition for kappa number is :

$$K_f = 0.225K_0$$

$$K_s = 0.675K_0$$

$$K_{floor} = 0.100K_0$$

$[OH^-]$: hydroxide concentration	(kg/m ³ liquor)
$[O_2]$: dissolved oxygen concentration	(kg/m ³ liquor)
T	: temperature	K
R	: universal gas constant	8.314 kJ/kmol.K
K_o	: inlet kappa number	

When they applied their model on data obtained on an industrial scale, they used an oxygen consumption rate of $\alpha=0.8$ kg(oxygen)/kg(lignin) without any tuning for the model.

They pointed out that a high reaction order with respect to lignin as proposed by some other workers gives abnormal reaction rates for high initial kappa number.

Myers and Edwards' [1989] model is applicable to a very wide range of operating conditions but it does not account for the cellulose degradation. Their model will be used for prediction of kappa number.

3.2.4 Iribarne and Schroeder model

The motivation of the Iribarne and Schroeder [1997] study was to find a global kinetic model which covered a higher range of oxygen partial pressure up to 18.4 MPa. The main

hypothesis of their study was that the higher the concentration of oxygen might increase delignification rates. Previous studies covered up to 1.5 MPa.

The Iribarne and Schroeder [1997] model covers a wide range of operating conditions from 20–60 for kappa number, up to a 20% consistency, 50°C to 150°C for temperature, 0 to 0.4 mole/litre for alkali concentration, 2 to 26 cp for viscosity and up to 18.4 MPa.

Iribarne and Schroeder [1997] expressed oxygen as concentration (mole/litre) in their model instead of using oxygen partial pressure. This is because the oxygen concentration in the liquid phase does not depend only on oxygen partial pressure but also on alkali concentration and temperature. As the alkali concentration and temperature increases, the oxygen concentration decreases. Iribarne and Schroeder [1997] used Broden and Simonson equations to estimate oxygen concentration in alkali medium

[Iribarne and Schroeder, 1997].

$$[O_2] = 5.351 - 1.252 * 10^{-2}T - 79.54P_{O_2} + 2.135 * 10^{-4}P_{O_2}T^2 + 2.125 * 10^4 \frac{P_{O_2}}{T} \quad (3.10)$$

where:

$[P_{O_2}]$: oxygen partial pressure MPa

$[O_2]$: dissolved oxygen concentration mol/litre

T : temperature °C

The kinetic model of lignin degradation is described by two first order differential equations in the kappa number.

$$-\frac{dK_f}{dt} = 6 \times 10^{11} e^{\frac{-67}{RT}} [OH^-]^{1.2} [O_2]^{1.3} K_s \quad (3.11)$$

$$-\frac{dK_s}{dt} = 6 \times 10^4 e^{\frac{-40}{RT}} [OH^-]^{0.3} [O_2]^{0.2} K_f \quad (3.12)$$

$$K_f(0) = 0.57K_0 \quad (3.13)$$

$$K_s(0) = 0.43K_0 \quad (3.14)$$

$[OH^-]$: alkali concentration in solution	mole/litre
$[O_2]$: oxygen concentration in solution	mmole/litre
K	: Kappa number	mL/g

The model predicts that initial delignification would be essentially complete in 7 minutes. The final delignification would be much slower.

The model assume stoichometric coefficient of $1.33 \times 10^{-3} g_{NaOH}/(g_{softwood})(\Delta K)$ for caustic soda consumption and almost the same amount for oxygen consumption.

Cellulose degradation

It is expressed as zero-order reaction in m_n .

$$\frac{dm_n}{dt} = 7 \times 10^{10} e^{\frac{-78}{RT}} [OH^-]^{0.3} [O_2]^{0.4} \quad (3.15)$$

$$DP_n = \frac{10^6}{162m_n} \quad (3.16)$$

$$DP_n = 961.38 \log_{10} \eta - 245.3 \quad (3.17)$$

$[OH^-]$: hydroxide concentration	mole/litre
$[O_2]$: oxygen concentration	mmole/litre
m_n	: number-average moles of cellulose per metric ton of pulp	mol/metric ton
η	: viscosity	mPa.s
DP_n	: degree of polymerization	

3.2.5 Gendron's model

Gendron *et al.* [2002] presents kinetic model for oxygen bleaching. The model covers lignin removal and cellulose degradation. The model was developed using unbleached pulp of specific inlet kappa number ($K = 32$). The conditions affecting the rate of lignin removal are:

1. Temperature (T).

2. Pressure (P).
3. Caustic feed flow rate.
4. Oxygen feed flow rate.

Weaknesses

1. High reaction order with respect to kappa number.
2. The experiments were carried out at one kappa number ($K = 32$)
3. The model fixed the alkali concentration
4. There are redundant variables; oxygen flow rate and pressure.
5. The model accounts for the pressure gradient which has a small effect compared with the effect of alkali charges and temperature [McDonough, 1986]

From 1 and 2, following the arguments of Iribarne and Schroeder [1997] and Myers and Edwards [1989], the model would not predict the kappa number correctly if it was different from 32. This will limit the capability of the delignification reactor to handle the variation in the digester outlet kappa number due to any upsets. It will be also difficult for the optimization of the digester and bleaching unit.

3.2.6 Agarwal and Genco model

Agarwal *et al.* [1998] presented a kinetic model for both kappa number and cellulose degradation.

Kappa number model:

$$-\frac{dK}{dt} = -6.59 \times 10^{-6} e^{-\frac{107.2}{RT}} [OH]^{0.92} P_{O_2}^{0.53} K^{7.7} \quad (3.18)$$

Cellulose degradation model:

$$\log\left(\frac{\eta}{\eta_0}\right) = -5.8265 \times 10^{-7} T^2 [OH]^{0.8} P_{O_2}^{0.2} \log(t) \quad (3.19)$$

$[OH^-]$: hydroxide concentration	g/litre
P_{O_2}	: oxygen pressure	N/m ²
t	: time	minutes
K	: Kappa number	ml
η	: intrinsic viscosity	cc/g
T	: temperature	°C

Agarwal *et al.* [1998] presented an equation to correlate the intrinsic viscosity to dynamic viscosity expressed in cP .

$$\mu(cP) = 0.0003\eta^2 - 0.392\eta + 175.7 \quad (3.20)$$

Weaknesses

1. High reaction order with respect to kappa number.
2. The experiments were carried out at one kappa number.
3. The model fixed the alkali concentration.
4. Equation 3.20 was fitted using Excel and it did not predict the data correctly at all and this is seemingly due to unscaled data used by Agarwal *et al.* [1998] to fit it. It is recommended that the data be scaled first before fitting.

3.2.7 Summary

From Table 3.1, both of the Myers and Edwards [1989] and Iribarne and Schroeder [1997] models cover a wide range of operating conditions. As a result, their models will be used in developing the dynamic model for a continuous industrial reactor. The Myers and Edwards

	Olm and Teder (1979)	Hsu and Hsieh (1988)	Myers and Edwards (1989)	Iribarne and Schroeder (1997)	Gendron (2001)
Initial Kappa	29.5	29.5	11 - 128	20 - 60	32
Consistency	0.3 to 8	0.4	Up to 30	10	10
Temperature, °C	110	75 - 125	75 - 105	50-150	90 - 110
Pressure, Mpa	0.98	0.4 - 1.1	0.14 - 1	0 - 18	0.34-0.69
Delignification Kinetics	✓	✓	✓	✓	✓
Cellulose Degradation Kinetics	✓			✓	✓

Figure 3.1: Comparison of the different models operating ranges

[1989] model will be used for the kappa number calculation and the Iribarne and Schroeder [1997] model will be used for cellulose degradation calculations. Table 3.1 summarizes the different kinetic models equations used in this comparison.

Table 3.1: Summary of global kinetic models

<p>Olm and Teder [1979]</p> $-R_K = A_1 e^{\frac{-10}{RT}} [OH^-]^{0.1} P_{O_2}^{0.1} K + A_2 e^{\frac{-15}{RT}} [OH^-]^{0.3} P_{O_2}^{0.2} K$ <p>For Cellulose $-R_m = A_3 e^{\frac{-40}{RT}} [OH^-]^{0.2} P_{O_2}^{0.8} + A_4 e^{\frac{-53}{RT}} [OH^-]^{0.6} P_{O_2}^{0.1}$</p> $\log m = 4.35 - 1.25 \log \eta$
<p>Hsu and Hsieh [1988]</p> $-R_K = 2.5 e^{\frac{-36}{RT}} [OH^-]^{0.8} P_{O_2}^{0.4} K^{3.1} [u(t) - u(t-2)]$ $+ 143.5 e^{\frac{-71}{RT}} [OH^-]^{0.7} P_{O_2}^{0.7} K_2^{3.1} [u(t-2)]$
<p>Myers and Edwards [1989]</p> $-R_{K_f} = 1.51 \times 10^5 e^{\frac{-31.6}{RT}} [O_2]_{liq}^{0.43} K_f$ $-R_{K_s} = 1.68 \times 10^7 e^{\frac{-61.4}{RT}} [OH^-]^{0.0875} [O_2]^{0.43} K_s$ $[O_2] = [O_2]_i - [O_2]_{used}$ $[OH] = [OH]_i - [OH]_{used}$ <p>$K_f = 0.225 K_i$ and $K_s = 0.675 K_i$</p>
<p>Agarwal <i>et al.</i> [1998]</p> $-\frac{dK}{dt} = -6.59 \times 10^{-6} e^{-\frac{107.2}{RT}} [OH]^{0.92} P_{O_2}^{0.53} K^{7.7}$ $\log\left(\frac{\eta}{\eta_0}\right) = -5.8265 \times 10^{-7} T^2 [OH]^{0.8} P_{O_2}^{0.2} \log(t)$
<p>Iribarne and Schroeder [1997]</p> $-R_K = 6 \times 10^{11} e^{\frac{-67}{RT}} [OH^-]^{1.2} [O_2]^{1.3} K_f + 6 \times 10^4 e^{\frac{-40}{RT}} [OH^-]^{0.3} [O_2]^{0.2} K_s$ <p>For cellulose degradation $-R_m = 7 \times 10^{10} e^{\frac{-78}{RT}} [OH^-]^{0.3} [O_2]_{O_2}^{0.4}$</p>
<p>Gendron <i>et al.</i> [2002]</p> $\frac{d[K]}{dt} = -3.51 \times 10^{-6} e^{\frac{6938}{T}} N^{1.32} X^{0.33} P^{0.4} [K]^8$ <p>For cellulose $-\frac{dN_c}{dt} = B e^{\frac{-E_C}{RT}} N^{b_N} X^{b_X} P^{b_P} N_c$</p> $DP = \frac{DP_0}{DP_0 - (DP_0) \frac{N}{N_0}}$ $\log_{10}(\eta) = \frac{1}{954} (325 + (\frac{1}{0.75} DP)^{0.905})$

3.3 Development of Dynamic Model for Oxygen Delignification Reactor

Optimal selection of operating conditions

We now apply the kinetic models developed above to the development of a dynamic model of a continuous oxygen delignification tower. Generally, the objective is to remove as much lignin as possible in order to minimize the consumption of costly chemicals in subsequent bleaching stages. However, the penalty for using oxygen to remove lignin is the weakening of the fibers. A second objective then consists of ensuring that the oxygen treatment does not weaken the pulp beyond some limit. As discussed earlier, the weakening of the fibers is closely associated to the amount of depolymerization suffered by the cellulose chains.

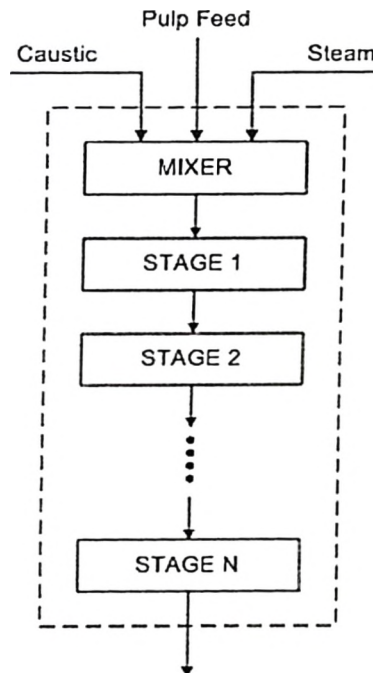


Figure 3.2: Modeling oxygen delignification reactor as a series of n CSTRs

3.3.1 Assumptions and model structures

1. Assume constant oxygen concentration through out the reaction due to its low solubility. Concentration in the liquid only drops towards zero when gas phase oxygen has been consumed [Pageau, 2000].
2. Assume constant operating pressure (no pressure drop).
3. Assume the reactor level is perfectly controlled.
4. The reactor will be simulated as series of CSTRs with constant volume $V = \frac{V_t}{n}$.
5. Assume adequate mixing within each CSTR.
6. Assume the density of the oven dry pulp is constant $\rho_{fibre} = 600$ g/litre.
7. Assume the heat capacity of the pulp mixture is constant.
8. Assume the density of the liquor is constant through the reactor $\rho_{liquor} = 1100$ g/litre.
9. Fast dynamics inside the steam mixer.
10. Oxygen contribution to the mass and energy balance is negligible comparing to the amount of pulp, caustic and steam.

3.3.2 Material and energy balance

Feed Mixer

Fast dynamics inside the mixer shown in Figure 3.3 will be assumed and so the mass and energy balance will be:

Total material balance:

$$F_0 = F_{in} + F_{NaOH} + F_{steam} \quad (3.21)$$

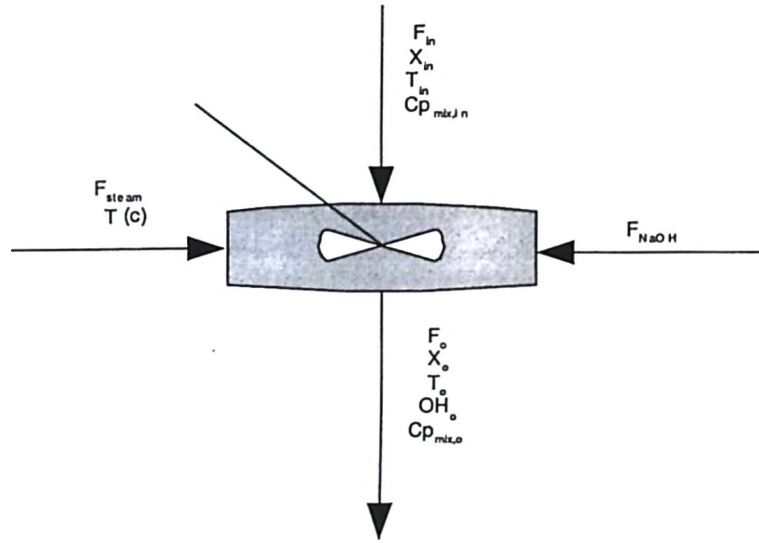


Figure 3.3: Feed Mixer

where:

F_{in} : Is the inlet pulp feed flow rate g/min

F_{NaOH} : Is the sodium hydroxide flow rate g/min

F_{steam} : Is the steam flow rate g/min

Consistency:

$$X_0 = \frac{F_{in} X_{in}}{F_0} \quad (3.22)$$

where X_0 represents consistency of the pulp in percentage.

$$X = \frac{\text{total flow rate of fibre in g/min}}{\text{liquor flow in g/min} + \text{total flow of fibre in g/min}} \quad (3.23)$$

$$\frac{1}{\rho_l} = \frac{1-X}{\rho_{liquor}} + \frac{X}{\rho_{Fibre}} \quad (3.24)$$

$$\text{Kappa number} = \frac{1}{0.147} \times 100[L] \quad (3.25)$$

where $[L]$ is the lignin mass fraction.

Component material balance:

$$[L]_o = [L]_{in} \quad (3.26)$$

$$[C]_o = [C]_{in} \quad (3.27)$$

where $[L]_o$ is the inlet lignin mass fraction and $[C]_o$ is the inlet cellulose mass fraction as follows:

$$[L] = \frac{\text{total mass of Lignin}}{\text{total mass of fibre (Lignin + Cellulose)}}$$

$$[C] = \frac{\text{total mass of Cellulose}}{\text{total mass of fibre (Lignin + Cellulose)}}$$

For Sodium hydroxide concentration:

$$[OH^-]_0 = \frac{[OH^-]_{in} F_{NaOH} / \rho_{NaOH}}{(1 - X_0) F_0 / \rho_{liq}} \text{ (mole/litre)} \quad (3.28)$$

where:

- ρ_{NaOH} : Is the density of the sodium hydroxide feed solution g/litre
 ρ_{liq} : Is the density of the liquor in the pulp stream g/litre

Total energy balance:

$$F_0 C_{P_{mix,o}} (T_0 - T_r) = F_{in} C_{P_{mix,in}} (T_{in} - T_r) + F_{NaOH} C_{P_w} (T_{in} - T_r) + F_{steam} (H_{T_s} - H_{T_r}) \quad (3.29)$$

where:

- T_r : Is the reference temperature K
 T_s : Is the superheated low pressure steam temperature K
 H_{T_s} : Is the steam specific enthalpy at T_s J/g
 C_{P_w} : Is specific heat of water J/g.K
 $C_{P_{mix,o}}$: Outlet pulp specific heat from the mixer J/g.K
 $C_{P_{mix,in}}$: Inlet pulp specific heat to the mixer J/g.K

Constants for the above are taken from Perry and Green [1997]

3.3.3 Reactor

Figure 3.2 presents the oxygen delignification reactor as an n series of CSTRs.

Material Balance:

Total material balance: for the n^{th} CSTRs, the total material balance as follows:

$$F_n = F_{n-1} \quad (3.30)$$

where:

F_n : Is the outlet flow rate from reactor n g/min

F_{n-1} : Is the inlet flow rate to reactor n g/min

Consistency:

$$\rho_{mix} V_{mix} \frac{dX_n}{dt} = F_{n-1} X_{n-1} - F_n X_n - \rho_{mix} V_{mix} \frac{d[L]}{dt} \quad (3.31)$$

where $\frac{dL}{dt}$ is the rate of delignification which can be expressed as the rate of decrease in kappa number per unit time. The amount of lignin removed is related to the kappa number governed by Equation (3.32).

$$[L] = \frac{0.147}{100} K \quad (3.32)$$

where $[L]$ is the residual lignin (mass fraction) and K is the kappa number. By substituting Equation 3.32 into Equation 3.31, the following consistency balance equation results:

$$\rho_{mix} V_{mix} \frac{dX_n}{dt} = F_{n-1} X_{n-1} - F_n X_n - 0.00147 \rho_{mix} V_{mix} X_n (R_f + R_s) \quad (3.33)$$

and for density:

$$\frac{1}{\rho_t} = \frac{1-X}{\rho_{liquor}} + \frac{X}{\rho_{pulp}} \quad (3.34)$$

where ρ_t is the total mixture density of the pulp and liquor, X is the consistency, ρ_{pulp} is the pulp density, assumed to be 600 g/litre.

Component material balance:

Lignin material balance: Delignification in bleaching is achieved through the combination of oxidation and alkaline extraction. The oxidants are chlorine, chlorine dioxide, sodium hypochlorite, oxygen and hydrogen peroxide. These oxidants react rapidly with lignin, resulting in changes in the structure and in fragmentation of the macromolecule of lignin in the unbleached pulp. Oxidation of the lignin not only breaks the bonds in the lignin macromolecule creating smaller more soluble fragments, it also spawns a new functional groups such as carboxylic acid and phenols. These functional groups increase the ionic character of lignin specially in alkali solution and make it more soluble in water. From these oxidants, oxygen is used in alkaline medium.

[Myers and Edwards, 1989] kinetic model is used for lignin removal. Myers and Edwards [1989] model is applicable to a very wide range of operating conditions. It can be used for both of softwood and hardwood kraft pulps. Also it can be used for all consistencies up to 30% pulps and initial kappa number range varying from 11 to 128.

$$\rho_t V \frac{d}{dt}(K_{f,n} X_n) = F_{n-1} X_{n-1} K_{f,n-1} - F_n X_n K_{f,n} - \rho_{mix} V_{mix} X_n R_f \quad (3.35)$$

$$\rho_t V \frac{d}{dt}(K_{s,n} X_n) = F_{n-1} X_{n-1} K_{s,n-1} - F_n X_n K_{s,n} - \rho_{mix} V_{mix} X_n R_s \quad (3.36)$$

$$R_f = 1.51 \times 10^5 e^{\frac{-31.6}{RT}} [O_2]^{0.43} K_f \quad (3.37)$$

$$R_s = 1.68 \times 10^7 e^{\frac{-61.4}{RT}} [OH^-]^{0.875} [O_2]^{0.43} K_s \quad (3.38)$$

where:

$$K = K_f + K_s + K_{floor} \quad (3.39)$$

$$R_f = \frac{g(\text{lignin})}{g(\text{o.d.pulp}) \cdot \text{min}} \quad (3.40)$$

The initial condition for kappa number is :

$$K_f = 0.225K_0$$

$$K_s = 0.675K_0$$

$$K_{floor} = 0.100K_0$$

K_0 is the inlet kappa number, K_f is the easily and rapidly removed lignin and K_s is the slowly removed lignin.

Cellulose material balance(carbohydrate degradation): Carbohydrate degradation is the chief factor limiting the amount of delignification achievable in the oxygen delignification stage [McDonough, 1986]. The more important component in the pulp is the cellulose since it is the major component in bleached pulp. Therefore, it is responsible for the strength of the pulp. Subsequently, cellulose will be studied. Cellulose consists approximately of 90.7% D-Glucose. The only repeating unit in cellulose polymer is Anhydro-D-glucose [Casey, 1980], with a molecular weight of 162 and with repeating units DP_n (degree of polymerization). Cellulose is attacked by free radicals generated by the oxygen. These free radicals randomly attack the cellulose chain and decrease the degree of polymerization.

Measuring the cellulose content is not possible online so the rate of cellulose degradation can be monitored by the change in viscosity with time. The number-average degree of polymerization is calculated as a function of viscosity using the Iribarne and Schroeder [1997] model as the following:

$$DP_n = 961.38 \log_{10} \eta - 245.3 \quad (3.41)$$

The cellulose degradation has been reported in literature in terms of the number of cellulose chains, m_n , which is the moles of cellulose per ton of pulp [Iribarne and Schroeder, 1997].

The material balance of cellulose is :

$$\rho_l V \frac{d}{dt}(m_{n,n} X_n) = F_{n-1} X_{n-1} m_{n,n-1} - m_{n,n} X_n F_n + \rho_l V X_n R_{m,n,n} \quad (3.42)$$

$$R_{m,n} = 7 \times 10^{10} e^{\frac{-78}{RT}} [OH^-]^{0.3} [O_2]^{0.4} \quad (3.43)$$

$$DP_n = \frac{10^6}{162 m_n} \quad (3.44)$$

$$R_m = \frac{g(\text{Cellulose})}{g(\text{o.d.pulp}) \cdot \text{min}} \quad (3.45)$$

Degree of polymerization is the number of anhydroD-glucose units in the cellulose polymer chain, It ranges from 600 to 1500 for commercial wood pulp [Watson, 1994]

Sodium hydroxide material balance:

Iribarne and Schroeder [1997] used an empirical equation to express the $[OH^-]$ consumed.

$$[NaOH]_{used} = 1.33 \times 10^{-3} \Delta K \times \text{flow of fiber(g/min)} \quad (3.46)$$

The material balance for sodium hydroxide is therefore:

$$\begin{aligned} \rho_{mix} V_{mix} / \rho_{liq} \frac{d}{dt} ((1 - X_n) [OH]_n) &= \frac{F_{n-1} (1 - X_{n-1})}{\rho_{liq}} [OH]_{n-1} - \frac{F_n (1 - X_n)}{\rho_{liq}} [OH]_n \\ &\quad - 1.33 \times 10^{-3} \frac{X_n \rho_{mix} V_{mix}}{M_{NaOH}} (R_f + R_s) \end{aligned} \quad (3.47)$$

Sodium hydroxide consumption is attributed only to the delignification reaction. There is no data to support the assumption of sodium hydroxide consumption by cellulose degradation which must be taken into account.

Oxygen material balance: Broden and Simonson equations will be used to estimate oxygen concentration in water; by this way we can take oxygen partial pressure into account for control purposes [Iribarne and Schroeder, 1997].

$$\begin{aligned}
[O_2] = & 5.351 - 1.252 \times 10^{-2}T - 79.54P_{O_2} + 2.135 \times 10^{-4}P_{O_2}T^2 \\
& + 2.125 \times 10^4 \frac{P_{O_2}}{T} \quad (\text{mmole/litre})
\end{aligned} \tag{3.48}$$

with temperature in Kelvin and P_{O_2} in MPa.

It is recommended to use oxygen concentration in the model instead of oxygen partial pressure because oxygen concentration is not only a function of oxygen partial pressure but also the temperature and the sodium hydroxide concentration.

Energy balance:

$$\begin{aligned}
\rho_{mix} V_{mix} C_P \frac{dT_n}{dt} = & F_{n-1} C_P T_{n-1} - F_n C_P T_n \\
& - 0.00147 \rho_{mix} V_{mix} X_n H_{rx} (R_f + R_s)
\end{aligned} \tag{3.49}$$

where H_{rx} is the Heat of reaction

3.4 Simulation Results

The nonlinear model developed was then applied to the Kushiro mill oxygen delignification reactor described in detail in Chapter 4. Step tests were performed in the oxygen delignification nonlinear model built in Simulink using S-functions to study the relationships between the inputs and the outputs. The Kushiro mill oxygen delignification reactor has a six trays. Each tray was considered as a single CSTR. It was assumed that the outlet kappa number and viscosity were directly measurable with no measurement delay.

Figure 3.4 shows the open loop response dynamics of the full order nonlinear model for a $-5K$ change in the reactor temperature. A decrease in the reactor temperature increases

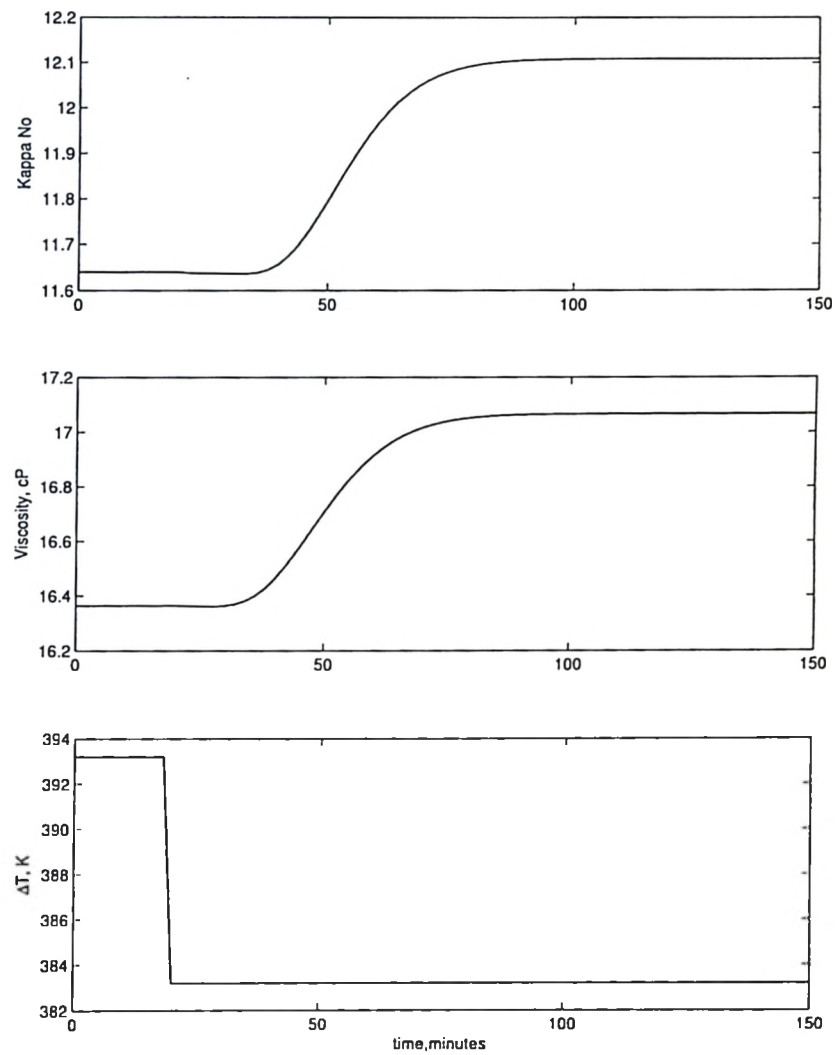


Figure 3.4: Step response of the outlet kappa number and outlet viscosity to step disturbance in the delignification reactor top temperature ($\Delta T = -5K$)

both viscosity and kappa number. Figures 3.5 and 3.6 show the responses to step changes in inlet kappa number and inlet caustic soda flow rate respectively. An increase in the inlet kappa number will increase the outlet kappa number and viscosity due to consumption of caustic soda while an increase in inlet caustic soda flow rate will decrease the outlet kappa number and viscosity.

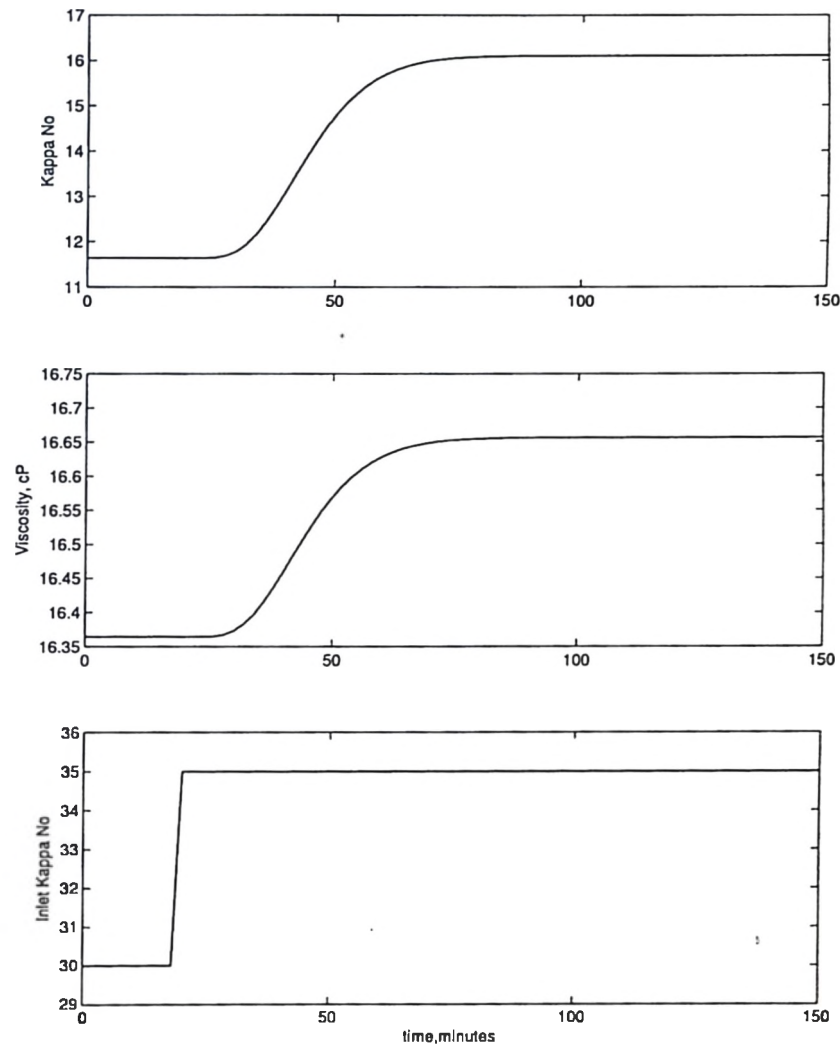


Figure 3.5: Step responses of the outlet kappa number and outlet viscosity to step disturbance in the delignification reactor inlet kappa number ($\Delta kappa = +5$)

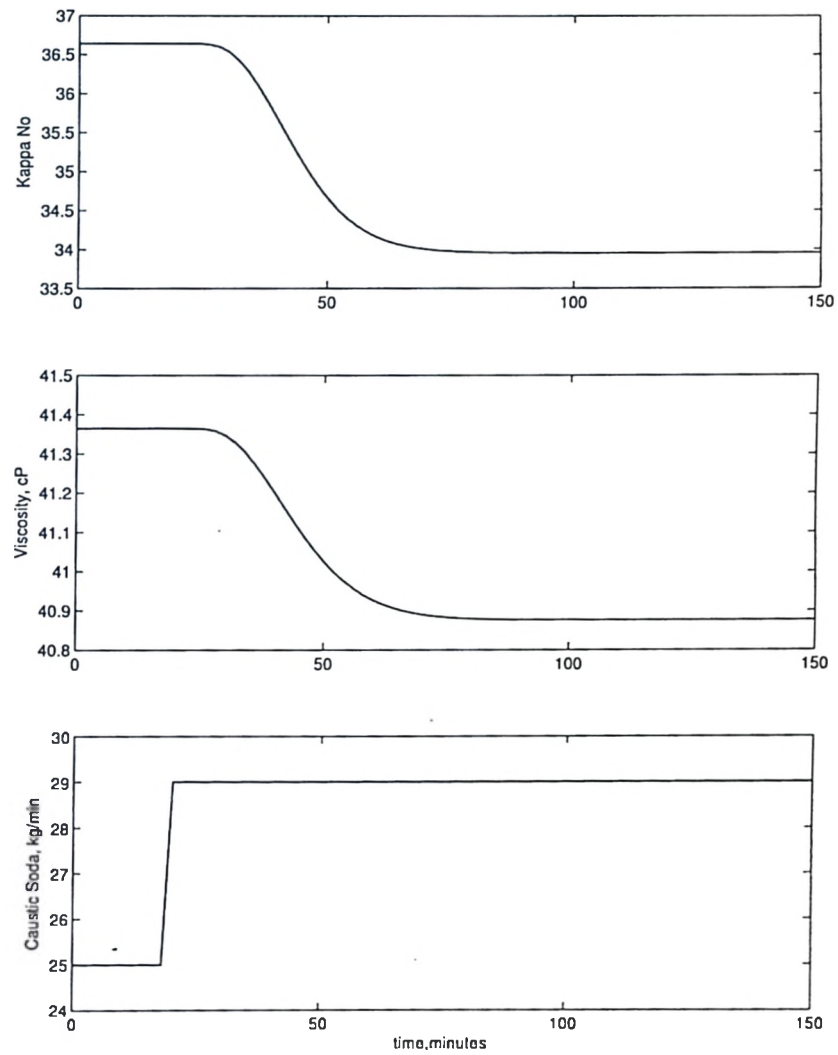


Figure 3.6: Step response of the outlet kappa number and outlet viscosity to +4 kg/ton change in the delignification reactor inlet caustic flow rate

Chapter 4

Model-Based Control of the Oxygen Delignification Unit

4.1 Introduction

The fundamental mass and energy balance model developed in Chapter 3 for an oxygen delignification reactor is configured to match the reactor inlet and outlet conditions for Jujo paper's Kushiro mill. The dynamic performance of model predictive control (MPC) on the developed model is evaluated. The dynamic real time optimization (DRTO) approach to track optimum operating point of a chemical plant developed in chapter 2 is also applied.

4.2 Kushiro Mill Oxygen Bleaching Unit

4.2.1 Kushiro mill overview

Jujo paper's Kushiro mill, with a newsprint production capacity of around 460000 tons per year is located in the eastern part of Hokkaido island in Japan [Sakum *et al.*, 1987]. A kraft pulp plant at Kushiro mill started operation in August 1975, and has replaced the former

high yield sulfite pulp line to provide reinforcing pulp for news print furnish. The needs to improve pulp quality, solve pollution problems and cope with change of wood species were the key reasons for this investment. Especially, a careful consideration was given to environmental protection and it was decided to employ various installations along with an oxygen delignification process.

Kushiro mill has softwood semi-bleached kraft pulp line with a design capacity of 320 tons per day. The line consists of a kaymr digester, a high consistency oxygen delignification tower and single sodium hypochlorite bleaching stage. The oxygen delignification tower is a reactor used for removing the maximum amount of lignin from the pulp before the bleaching plant.

The main equipment units are:

- Kaymr vapor/liquid phase digester with 2.5 hours of high-heat washing zone.
- Diffuser washer
- Pressure knotter
- Drum washer
- Suction mold with pressure roll and vacuum pump.
- Steam mixer
- High density pump
- Kaymr oxygen delignification reactor with a fluffer and 6 trays
- Two drum washers in series.
- Hypochlorite bleaching tower.
- Screen room

4.2.2 Oxygen bleaching unit process description

After the brown stock washing stage, magnesium oxide is added as a protector to the pulp at the mixing chest. The pulp is then pumped to a suction mold, where the pulp is dewatered to 25 to 27 % consistency with a good stability. After the suction mold, the pulp is shredded,

and alkaline solution NaOH is added. Under normal operation, the kappa number after the oxygen stage is controlled by the alkaline addition. Following alkaline addition, the pulp is preheated to 65°C with low pressure steam at the steam mixer.

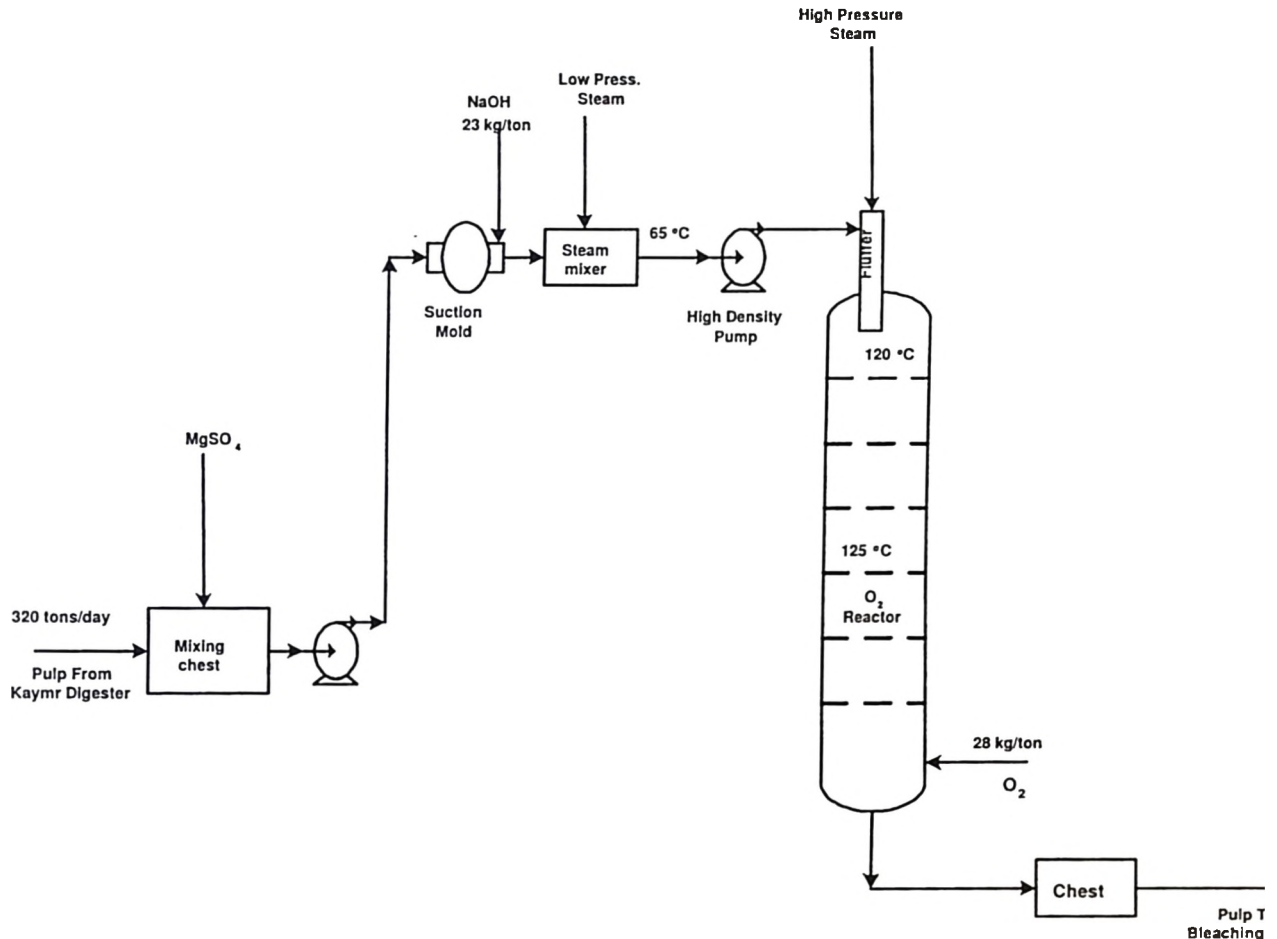


Figure 4.1: Jujo Mill oxygen bleaching line

Thereafter, the pulp is transported by means of a high density pump to a reactor through a fluffer. The reactor has six trays, and the retention time is controlled with the rotating speed of a shaft. The delignification reactor operating conditions are described in Table 4.1. The temperature at the top of the reactor is maintained at 120 °C by high pressure steam. The temperature at the middle of the reactor shows 125 °C. Oxygen gas (28 kg/ton) is fed from under the lowest tray, and the reactor pressure is maintained at 6.5 kg/cm²-gauge with

relief venting of exhaust gas. The oxygen content based on dry gas is 90% at the bottom and 75% at the top of the reactor. At the bottom of the reactor, the pulp is diluted to about 3% consistency before being transported to a blow tank. The oxygen delignified pulp is then washed in two drum washers in series and sent to the hypochlorite bleaching stage, where it is bleached with sodium hypochlorite to 60-65% brightness.

Table 4.1: Jujo Mill oxygen bleaching line operating conditions

Variables	Value
Production rate	320 AD ton/day
Pulp consistency in the reactor	23-25%
Temperature at the top	120 °C
Temperature at the middle	125 °C
Total Pressure	6.5 kg/cm ² -gauge
O ₂ partial pressure	3.5 kg/cm ² -gauge
NaOH flow rate	23 kg/ton
MgO flow rate	1 kg/ton
O ₂ flow rate	28 kg/ton
Inlet kappa number	30
Outlet kappa number	12
Inlet Viscosity	19.5 cP
Outlet viscosity	16 cP

The viscosity of the oxygen delignified pulp was reported to be 16 cP. Magnesium oxide is very effective against cellulose degradation. Without magnesium oxide, the pulp would drop to 11 cp.

Controlled Variables

The main considered variables in this study are:

1. Kappa number
2. Pulp Viscosity

The main objective is to minimize the outlet kappa number and to control its variation before the bleaching plant. Controlling this variation will reduce the operating cost of the downstream units. It is also required to keep the viscosity between limits.

Manipulated Variables

The most important variables affecting oxygen delignification are:

1. Caustic soda flow rate
2. Reactor Temperature – The temperature in the reactor is controlled mainly by the high pressure steam.
3. Oxygen partial pressure or concentration in the liquor phase – It is desirable to keep P_{O_2} constant by manipulating the inlet oxygen flow rate and the vent stream to the atmosphere.

Process Disturbances

From many disturbances that can affect the oxygen bleaching process such as inlet kappa number, production rate and oxygen partial pressure, the inlet kappa number is the major disturbance and will be selected for this study.

4.3 Model-Based Control

The control objective was to maintain the outlet kappa number and viscosity at their set points by manipulating the reactor temperature set point and inlet caustic rate. The reactor temperature is being controlled using a local PID controller by manipulating the steam flow rate. Disturbances considered were changes inlet kappa number of the pulp feed. Step tests were performed on the model and linear dynamic relationships between the inputs and outputs identified. MPC studies were conducted using the Matlab MPC Toolbox on the linearized models.

4.3.1 Linear dynamic model identification

Step tests were performed in the oxygen delignification nonlinear model built in Simulink using S-functions to identify the linear relationships between the inputs and the outputs. Applying step changes in the manipulated variables, a low-order transfer function model was generated. The reaction curves were used to fit First-Order-Plus Time-Delay (FOPTD) transfer functions as shown in Equation 4.1.

$$\begin{bmatrix} y_k \\ y_{vis} \end{bmatrix} = \begin{bmatrix} \frac{-0.7}{13s+1} e^{-13.6s} & \frac{-0.029}{13s+1} e^{-24s} \\ \frac{-0.123}{14s+1} e^{-13.8s} & \frac{-0.08}{14.5s+1} e^{-18.5s} \end{bmatrix} \begin{bmatrix} u_{OH} \\ u_T \end{bmatrix} + \begin{bmatrix} \frac{0.83}{13s+1} e^{-14s} \\ \frac{0.06}{13.3s+1} e^{-14.5s} \end{bmatrix} D_k \quad (4.1)$$

The open loop response dynamics of the full order nonlinear model for changes in the reactor temperature, inlet kappa number and inlet caustic soda flow rate is shown in Figures 3.4, 3.5 and 3.6 respectively in Chapter 3.

4.3.2 Simulation results of model-based control

Model predictive control studies were conducted using the Matlab MPC Toolbox for the nonlinear oxygen delignification plant represented as Simulink S-functions. Figure 4.2 shows the Simulink interface for the simulation where the MPC is represented by nlmcsim block.

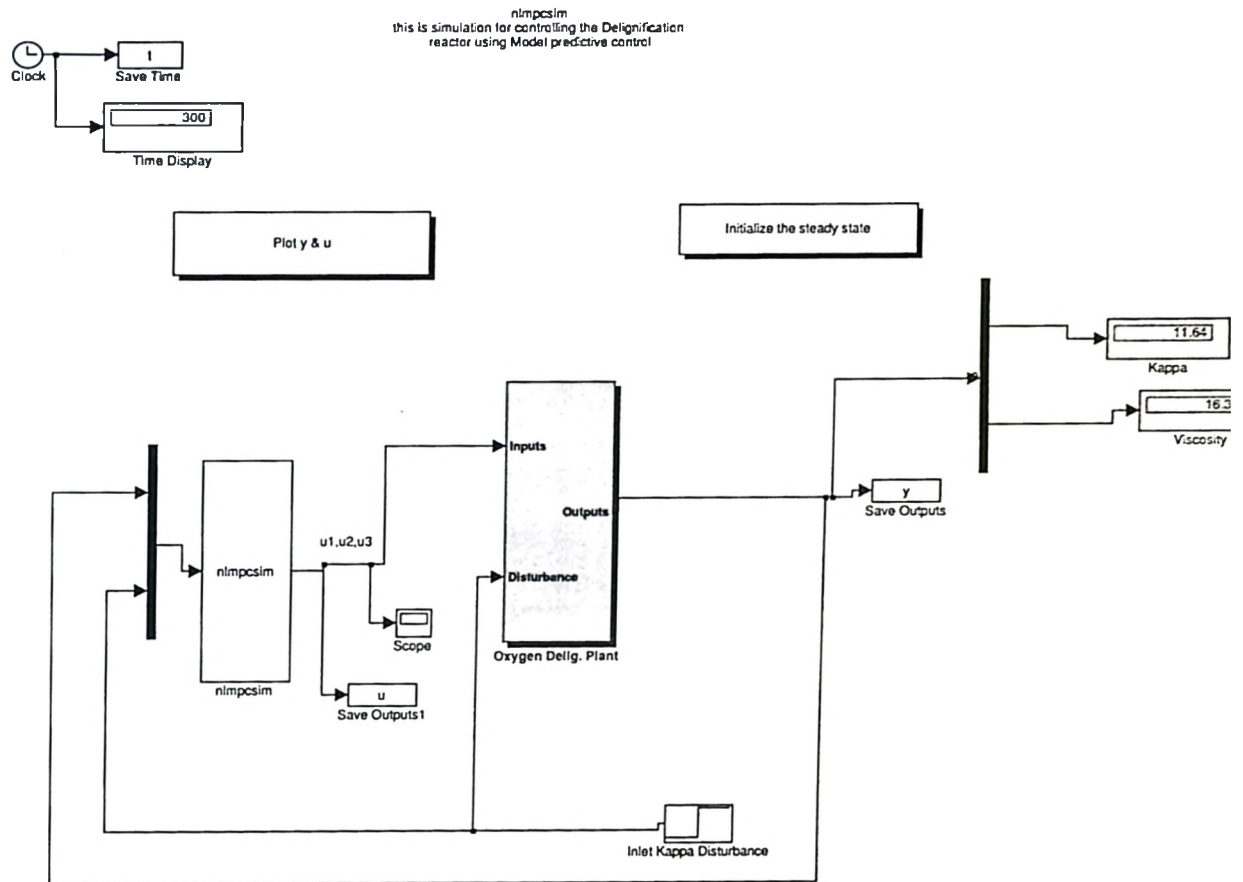


Figure 4.2: Model Predictive control simulation using a nonlinear plant

The tuning parameters comprising the objective function weighting matrices, the output prediction horizon and input control moves are selected and assumed constant as described in the Table 4.2. A sampling time of 2 minutes was used and the simulation horizon chosen to be 300 minutes.

parameters	Description	Value
M	Control moves horizon	2
P	Prediction horizon	15
N_S	Simulation horizon	151
Γ	Controlled variables weighting	I
Λ	Manipulated variables weighting	$\begin{pmatrix} 1.8 & 0 \\ 0 & 0.25 \end{pmatrix}$

Table 4.2: MPC tuning parameters

Control variables set-points were as follows:

Outlet kappa number = 11.6

Outlet viscosity = 16.4 cP

4.3.3 Disturbance rejection

Figures 4.3 and 4.4 show the system's closed-loop response to step changes in the inlet kappa number of a +3 and -3 respectively. The figures show good disturbance rejection with a modest amount of control effort.

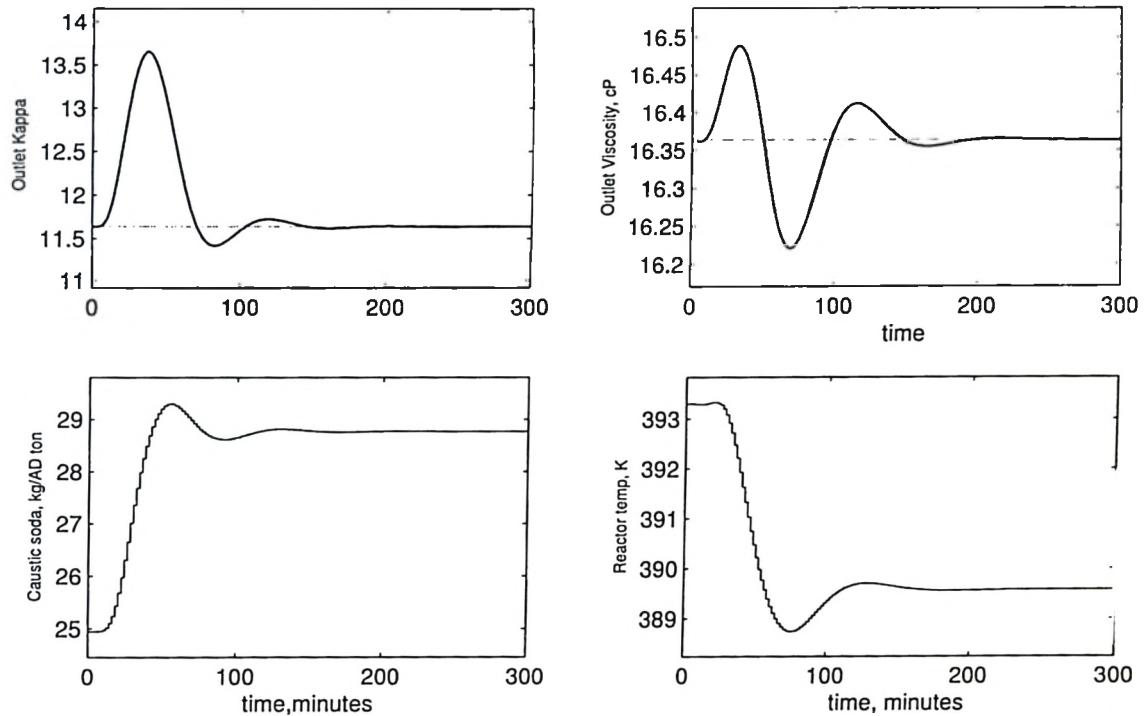


Figure 4.3: Closed-loop responses of the outlet kappa number and outlet viscosity, for step disturbances in the delignification reactor inlet kappa number (+3)

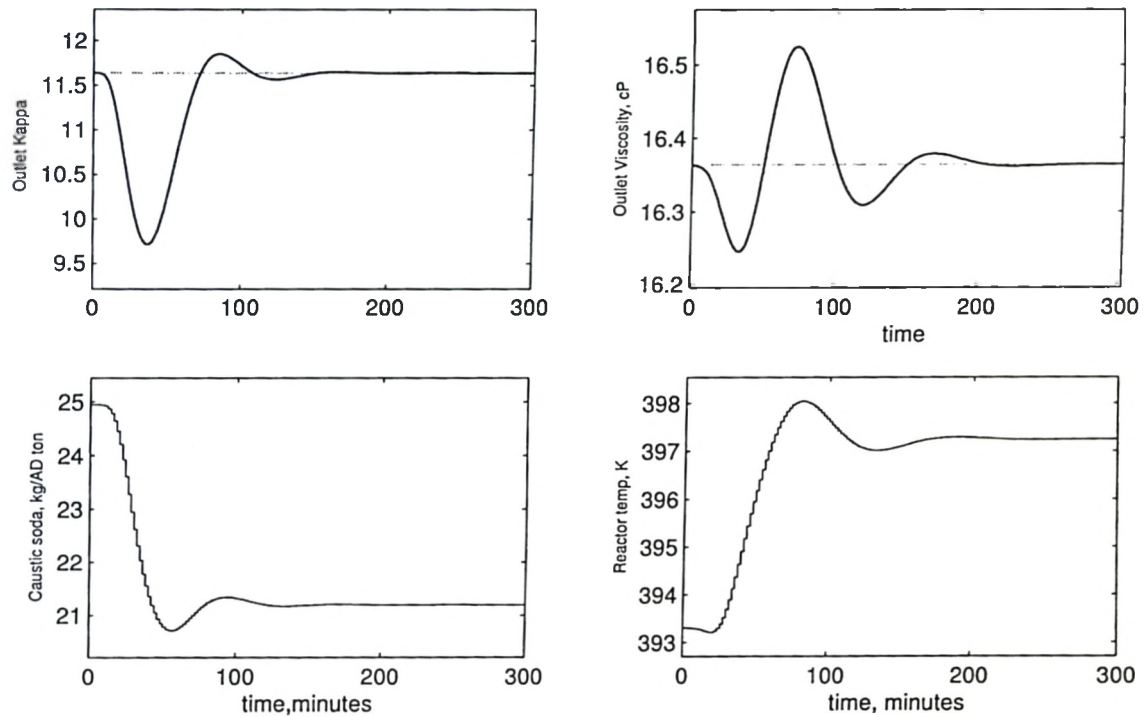


Figure 4.4: Closed-loop responses of the outlet kappa number and outlet viscosity, for step disturbances in the delignification reactor inlet kappa number (-3)

4.3.4 Set-point change

Figure 4.5 shows the system's closed-loop response to a set-point change of +1 in the outlet kappa number.

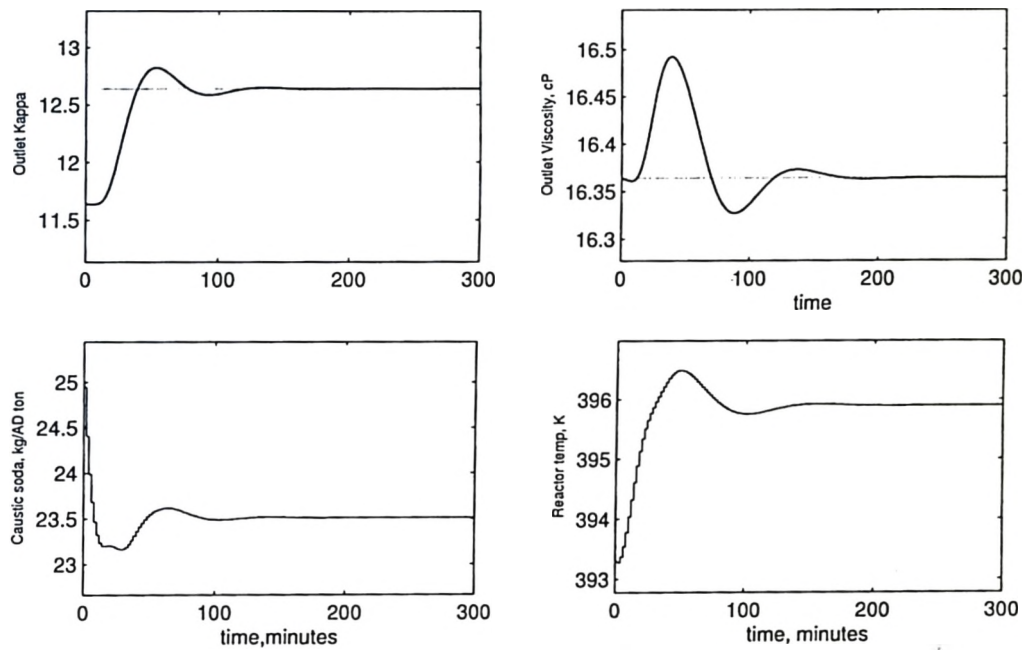


Figure 4.5: Closed-loop responses of the outlet kappa number and outlet viscosity, for set-point change of +1 in the outlet kappa number

Figure 4.6 shows the system's closed-loop response to step changes in the outlet kappa number and viscosity of +0.5 and -0.5 cP respectively.

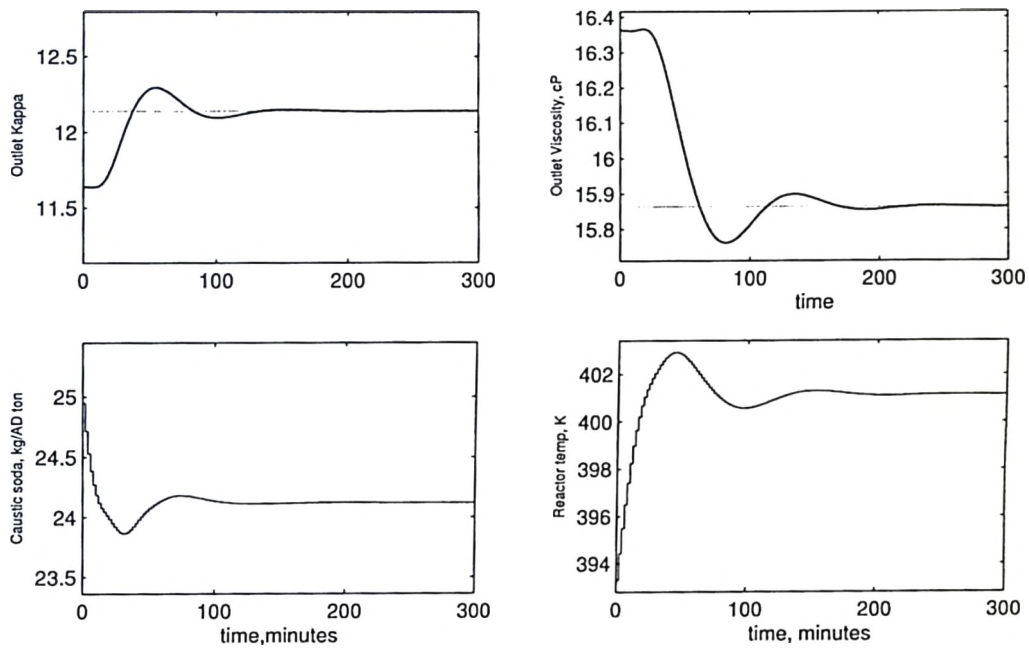


Figure 4.6: Closed-loop responses of the outlet kappa number and outlet viscosity, for set-point change of +0.5 in the outlet kappa number and -0.5 cP in the outlet viscosity

4.4 Interaction Between RTO and MPC Effect of Closed-Loop Dynamics

The MPC tuning parameters are selected and assumed constant as described in the Table 4.3. A sampling time of 3 minutes was used and the simulation horizon chosen to be 120 minutes.

parameters	Description	Value
M	Control moves horizon	2
P	Prediction horizon	15
N_S	Simulation horizon	41
B	large constant	70
$\Delta y_{k(sp)}$	change in kappa set-point	0
$\Delta y_{vis(sp)}$	change in viscosity set-point	0
Γ	Controlled variables weighting	I
Λ	Manipulated variables weighting	$\begin{pmatrix} 0.2 & 0 \\ 0 & 0.1 \end{pmatrix}$

Table 4.3: MPC tuning parameters

Control variables target set-points were as follows:

$$\text{Outlet kappa number} = 13$$

$$\text{Outlet viscosity} = 16.4 \text{ cP}$$

Steady-state relation ship between the inputs and the outputs

The steady-state model relating the manipulated inputs and controlled outputs was taken as follows:

$$\begin{bmatrix} y_{k_{ss}} - \bar{y}_{k_{ss}} \\ y_{vis_{ss}} - \bar{y}_{vis_{ss}} \end{bmatrix} = \begin{bmatrix} -0.7 & -0.029 \\ -0.123 & -0.08 \end{bmatrix} \begin{bmatrix} u_{OH_{ss}} - \bar{u}_{OH_{ss}} \\ u_{T_{ss}} - \bar{u}_{T_{ss}} \end{bmatrix} + \begin{bmatrix} 0.83 \\ 0.06 \end{bmatrix} \Delta d \quad (4.2)$$

where:

- y_k : Outlet kappa number
- y_{vis} : Outlet viscosity, cP
- u_{OH} : Inlet caustic flow rate, kg/ton
- u_T : Reactor temperature, K
- ss : Refer to the steady-state
- \bar{y} : Refers to the initial output steady-state
- \bar{u} : Refers to the initial input steady-state

Constraints: The operating variables constraints were not available in the original work, thus the model constraints limits will be assumed as follows:

$$\begin{aligned} 9 &\leq y_k \leq 13 \\ 14 &\leq y_{vis} \leq 19.5 \text{ cP} \\ 0 &\leq u_{OH} \leq 35 \text{ kg/ton} \\ 375 &\leq u_T \leq 402 \text{ K} \end{aligned}$$

Simulation Results

MIQP/Cplex is used for simulating the oxygen delignification reactor. The number of continuous variables was 2357 and the integer variables was 336.

Simulation results for small disturbances

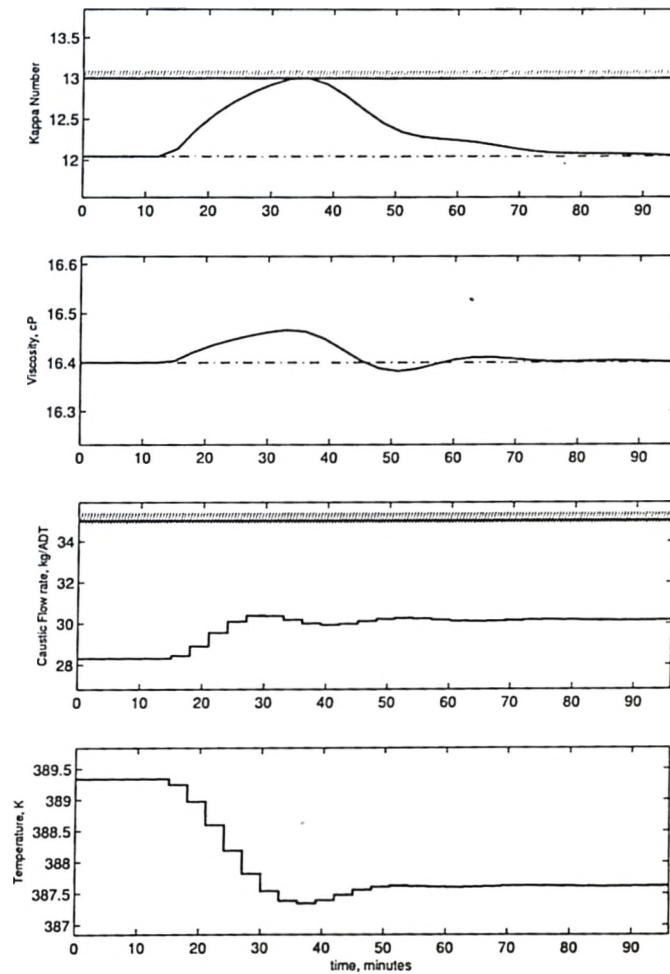


Figure 4.7: Non of the manipulated variables are saturated

Fig 4.7 shows the effect of a small disturbance (step change in inlet kappa number = 1.5). None of the manipulated variables are saturated. Only the kappa number is touching the upper constraint and it has to be backed-off to 12.

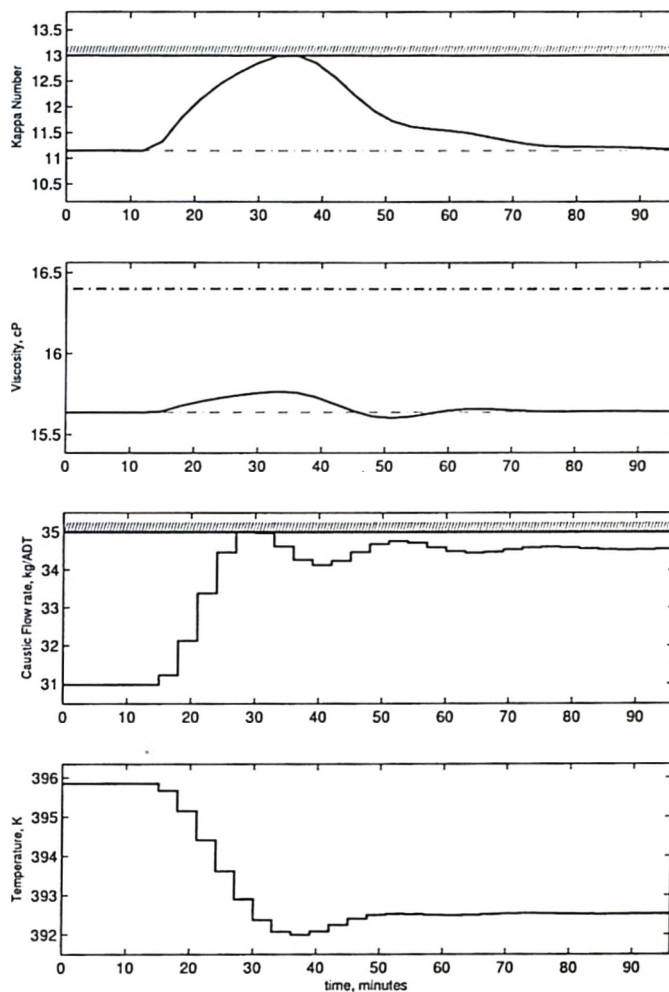
Step change in inlet feed kappa number=2.9

Figure 4.8: Output response to a step change in inlet kappa number of 2.82.

In Figure 4.8, the caustic soda flowrate is partially saturated. The kappa number set-point is backed-off from 13 to 11.2. The outlet kappa number is touching the upper bound while the outlet viscosity is within limits.

Chapter 5

Conclusions and Recommendations

5.1 Conclusions

A method to track the optimum of the chemical process such that violation of constraints can be prevented (Dynamic Real-Time Optimization) by inclusion of closed loop dynamics in Real Time Optimization was developed. Constrained model predictive control will be used as the regulatory control.

The Dynamic Real-Time Optimization (DRTO) problem was formulated here as a multilevel program where the upper and lower-level problems have a quadratic objective function with linear constraints and the lower-level optimization problems have quadratic objective functions that are strictly convex with linear constraints.

In this thesis also, a first-principles dynamic model of an oxygen delignification tower is developed. It is based on material and energy balances, and incorporates literature-based kinetic models for the lignin removal and cellulose degradation. The model produces steady-state results that are consistent with reported operating data. The model was used to generate approximate, linear dynamic relationships that were used in a model-based control strategy that yielded good closed-loop performance

5.2 Recommendations

1. In Dynamic real-time optimization study, the disturbance is assumed to be measured or estimated. This is not always the case in reality. Therefore this work needs to be extended to include estimation for the unmeasured disturbances.
2. Alternative computation strategies are required for dynamic real-time optimization to be developed in order to handle large MIMO systems because standard algorithms are not suitable particularly when the number of the integer variables increases. An interior point approach and more efficient branch and bound strategy might be used.
3. It is recommended to incorporate the calculations of target set-points from the Real-Time Optimization.
4. Further extensions to dynamic real-time optimization approach include the parameter uncertainties, model errors, process model mismatch and nonlinearities.
5. Further study for the oxygen delignification reactor should consider the incorporation of an inferential strategy to estimate oxygen delignification outlet stream viscosity and kappa number from typically available measurements.

List of References

- AGARWAL, S. B., COLE, B. J. W., AND GENCO, J. M. (1998). Medium consistency oxygen delignification and tower design. *Aiche Symposium Series*, **94**(319), 32–46.
- ANSARI, R. M. AND TAD, M. O. (2000). Constrained nonlinear multivariable control of a fluid catalytic cracking process. *Journal of Process Control*, **10**, 539–555.
- BANDONI, J., ROMAGNOLI, J., AND BARTON, G. (1994). Optimizing control and the effect of disturbances: Calculation of the open-loop backoffs. *Computers and Chemical Engineering*, **18**(suppl), S505–S509.
- BARD, J. AND MOORE, J. (1990). A branch and bound algorithm for the bilevel programming problem. *siam J. Sci. Stat. Comput.*, **11**, 281–292.
- BARD, J. F. (1998). *Practical bilevel optimization: Algorithms and applications*. Kluwer Academic publishers, first edition.
- BECERRA, V., ROBERTS, P., AND GRIFFITHS, G. (1998). Novel developments in process optimization using predictive control. *J.Proc. Control*, **8**(2), 117–138.
- BEQUETTE, B. W. (2000). *Process Control, Modelling, Design and Simulation*. Prentice Hall International Series.
- BRENGEL, D. AND SEIDER, W. (1992). Coordinated design and control optimization of nonlinear processes. *Computers Chem. Engng.*, **16**(9), 26.
- CASEY, J. P. (1980). *Pulp and paper chemistry and chemical technology*, Vol. 1. John Wiley and Sons, New York, third edition.

- CLARK, P. A. AND WESTERBERG, A. W. (1990). Bilevel programming for steady-state chemical process design. i. fundamentals and algorithms. *Comput. Chem. Eng*, **14**(1), 87–97.
- FORTUNY-AMAT, J. AND MCCARL, B. (1981). A representation and economic interpretation of a two-level programming problem. *Journal of Operational research society*, **32**(9), 783–792.
- GAMS, D. C. (1998). *GAMS USER'S GUIDE*. GAMS Development Corporation, Washington D.C., gams 21.4 edition.
- GARCIA, C. E. AND MORSHEDI, A. M. (1986). Quadratic programming solution of dynamic matrix control QDMC. *Chem. Eng. Commun*, **46**, 73–87.
- GARCIA, C. E., PRETT, D. M., AND MORARI, M. (1989). Model predictive control: Theory and practice – a survey. *Automatica*, **25**(3), 335–348.
- GENDRON, S., BOUCHARD, J., AND BERRY, R. (2002). Optimal selection of operating conditions for an oxygen delignification tower. In *IPBC Proceedings*. IPBC, TAPPI PRESS.
- GROSDIDIER, P., MASON, A., AITOLAHTI, P. H., AND VANHAMAKI, V. (1993). FCC unit reactor-regenerator control. *Computers Chem. Engng*, **17**(2), 165–179.
- GROSSMANN, I. E., VISWANATHA, J., VECCHIETTI, A., RAMAN, R., AND KALVELAGEN, E. (2004). *DICOPT: A Discrete Continuous Optimization Package*. GAMS Development Corporation, Washington D.C., gams 21.4 edition.
- HSU, C. L. AND HSIEH, J. S. (1988). Reaction Kinetics in Oxygen Bleaching. *AICHE Journal*, **34**(1), 116–122.
- IRIBARNE, J. AND SCHROEDER, L. R. (1997). High pressure oxygen delignification of kraft pulp. *Tappi Journal*, **80**(10), 241–250.
- KASSIDAS, A. (1993). Model predictive control design with implicit economic criteria. Master's thesis, McMaster University.

- LOEBLEIN, C. AND PERKINS, J. (1996). Economic analysis of different structures of on-line process optimization systems. *Computers and Chemical Engineering*, **20**, S551-S556.
- LOEBLEIN, C. AND PERKINS, J. (1999). Structural design for on-line process optimization: I. dynamic economics of mpc. *AIChE Journal*, **45**(5), 1018-1029.
- MARLIN, T. E. (2000). *Process Control: designing processes and control systems for dynamic performance*. McGrawHill; second edition.
- MCDONOUGH, T. J. (1986). Oxygen bleaching processes. *Tappi Journal*, **69**(6), 46-49.
- MYERS, M. R. AND EDWARDS, L. L. (1989). Development and verification of a predictive oxygen delignification model for hardwood and softwood kraft pulp. *Tappi Journal*, **72**(9), 215-219.
- MYERS, M. R. AND EDWARDS, L. L. (1989). Development and verification of a predictive oxygen delignification model for hardwood and softwood kraft pulp. *Tappi Journal*, **72**(9), 215-219.
- NATH, R. AND ALZEIN, Z. (2000). On-line dynamic optimization of olefins plants. *Computers and Chemical Engineering*, **24**, 533-538.
- OLM, L. AND TEDER, A. (1979). The kinetics of oxygen bleaching. *Tappi Journal*, **62**(12), 43-46.
- PAGEAU, G. L. (2000). Two Stage Oxygen Delignification Controls Optimized for constant Kappa output. *Control Systems 2000*, , 117-122.
- PERRY, R. H. AND GREEN, D. W. (1997). *Perry's chemical engineering handbook*, Vol. seven. seventh edition.
- QIN, S. J. AND BADGWELL, T. A. (2003). A survey of industrial model predictive control technology. *Control Engineering Practice*, **11**(7), 733-764.
- SAKUM, S., IWASE, H., AND SOTOBAYASHI, H. (1987). H.c. oxygen bleaching with P.S.A. (low purity oxygen). In *1987 International Oxygen Delignification Conference*, pp. 141-144.

-
- WATSON, E. (1994). *Mathematical modelling and experimental study of kinetics of the acid sulphite pulping of eucalyptus wood*. PhD thesis, University of Natal, Department of Chemical Engineering.
- ZANIN, A., TVRZSK DE GOUVA, M., AND ODLOAK, D. (2002). Integrating real-time optimization into the model predictive controller of the FCC system. *Control Engineering Practice*, 10(8), 819–831.
-

Thode
TP
155.7
.575
2004
c.2